Inelastic scattering of protons by rare-earth nuclei

A. B. Kurepin

Nuclear Research Institute,
Academy of Sciences of the USSR, Moscow
Fiz. El. Chast. Atom. Yad., 5, 892-954 (October-December 1974)

A review is presented of investigations of inelastic scattering of protons of energy higher than 10 MeV with excitation of low-lying collective levels of rare-earth nuclei. Theoretical analysis methods with allowance for the strong coupling of the channels, including approximate methods, are considered. Attention is called to new possibilities afforded by such an analysis, especially when polarized protons are used. The optical-potential parameters for the scattering of protons by spherical and deformed nuclei are given, as are the deformation parameters obtained in studies of electromagnetic processes and of the scattering of protons, deuterons, and α particles.

INTRODUCTION

The possibility of obtaining information on the properties of nuclei in ground and excited states from data on the scattering of protons and light nuclei by nuclei depends considerably on the extent to which the interaction process that leads to excitation of the nuclei is known. A widely known method is that of Coulomb excitation, in which the inelastic scattering of charged particles with energy lower than the Coulomb barrier of the nuclei is due entirely to electromagnetic interaction. This process, however, yields information only on quantities connected with the Coulomb field of the nucleus. Nuclear effects become manifest in scattering when the energies of the incident charged particles are increased or when neutrons are scattered.

The most widely used method of approximating the nuclear interaction is by introducing a complex optical potential, which makes it possible to take effective account of the absorption, i.e., of the discarded channels of inelastic scattering and reactions. An appreciable amount of experimental data on inelastic scattering of protons by nuclei, in a wide range of energies, has been systematized in ref. 1, where a spherically symmetrical optical potential was used.

In the generalized optical model used to describe the inelastic-scattering process, one introduces a deviation of the potential from spherical, as a result of which collective levels of the target nuclei become excited in the inelastic scattering. As a rule, a strong coupling exists between these collective states and can be either direct or indirect (multistep). The inelastic elastic-scattering channels are therefore coupled with one another, and this leads to a system of coupled Schrödinger equations.[2,3]

The elastic-scattering channel is also coupled with the inelastic-scattering channels, and if this coupling is strong enough the elastic scattering cannot be analyzed without taking the inelastic-scattering channels into account. In other words, the optical-potential parameters determined only from data on elastic scattering by nuclei having strongly excited collective states, e.g., rotational states, should differ from the average set of parameters for spherical nuclei.[1] The effect of the inelastic-scattering channels on the elastic-scattering channel can be represented as a rescattering in the input channel, which is an effect of second or higher order. Consequently these processes cannot be accounted for in the usual distorted-wave method.

Although the model of strong coupling of channels with a nonspherical potential is sometimes suitable even in the case of scattering by light nuclei, it is most consistent to use it to describe inelastic scattering of protons and other charged particles by heavy nuclei. Indeed, the collective character of the low-lying states of these nuclei has been established from an analysis of the probabilities of the electromagnetic transitions and of the sequence of the low-lying levels. Therefore the methods developed for solving the system of coupled equations, the role of the various approximations used in the calculation, and the verification of the applicability of the simplest collective models to the description of excited states of nuclei should all be primarily verified when investigations are made of inelastic scattering of charged particles by heavy nuclei. Although the use of charged particles complicates the calculations somewhat, it offers advantages of a purely experimental character over neutron scattering. The levels of the heavy nuclei are so close together that the energy resolution presently obtained in experiments with neutrons is insufficient for detailed measurements of the angular distributions.

When describing elastic and inelastic scattering of medium-energy particles by heavy nuclei one can neglect the compound-nucleus formation mechanism, thereby greatly simplifying the calculations. The number of channels for the decay of the states of the compound nucleus is large in this case, and the probability of decay in any particular selected scattering channel is much smaller than the probability of the direct process described in accordance with the generalized optical model.

A number of years have elapsed since the publication of the review article by Tamura[4] and the papers of S. I. Drozdov,[5] devoted to the development of the method of coupled channels as applied to the scattering of particles with excitation of collective states of nuclei. During that time, new experiments were reported, performed with higher accuracy and made possible by working with beams of high energy resolution, by using single-isotope targets, by improving the experimental procedure, and by using semiconductor charged-particle detectors. In connection with the increased operating speed and memory volume of the computers, new calculation programs were accordingly developed, in which unnecessary approximations were eliminated, the required refinements in the type of interaction were introduced, and the number of considered scattering channels was increased. Particular attention was paid to the writing of programs suitable for rapid

reduction of the experimental data, particularly search programs based on least squares.

This article is an attempt to systematize the experimental data on inelastic scattering of protons, deuterons, and α particles, mainly by rare-earth nuclei. Various employed calculation methods are compared, the results of the analysis of the experimental data are discussed, and the nuclear deformation parameters obtained in various studies are compared.

Included among the experimental investigations of recent years are those by the present author and co-workers, who proposed and used a comparative method of investigating the inelastic scattering of protons.[6-8] The method consists of measuring the angular distributions of the cross sections, polarizations, asymmetry, and spin-flip probability, and also theoretical calculations for transition-region nuclei that differ little in charge and atomic weight but differ greatly in their collective properties. Such an abrupt transition from spherical to deformed nuclei (sudden appearance of static deformation) occurs in the isotopes of samarium when the number of neutrons changes from 88 to 90. The near equality of the atomic masses of the isotopes gives grounds for assuming that their optical-potential parameters differ little. The difference between the measured characteristics of elastic and inelastic scattering can be attributed only to a change in the character and in the coupling of the channels with changing collective properties of the target nuclei.

Even in the first measurements of the angular distributions of the scattering of 12-MeV protons by ^{148,154}Sm nuclei,[6] notice was taken of an interesting isotopic effect, namely, the oscillations in the angular distributions of elastic and inelastic scattering with excitation of the first 2^+ levels are much more pronounced for scattering by the spherical nucleus ^{148}Sm. An analogous effect for samarium nuclei was described in ref. 9; it was observed also in the much smoother region of the transition from the deformed to the spherical nuclei of the platinum isotopes.[10] The recently observed strong difference between the angular distributions of the asymmetry of inelastically scattered polarized 24.5-MeV protons[8] by ^{148,152}Sm nuclei is of interest for the determination of whether the excitation is rotational or vibrational. In the analysis of the angular distributions by the coupled-channel method, the accuracy of the determined interaction parameters of the optical potential and of the quadrupole and hexadecapole deformation increased by measuring the angular distributions of the inelastic scattering of protons with excitation of a number of levels [0^+, 2^+, 4^+, (6^+)] of the ground-state rotational band at different proton energies and by determining the polarization and asymmetry in the scattering of polarized protons. All this increases the number of equations but keeps the number of parameters constant, if we neglect the smooth dependence of several of the optical-potential parameters on the energy.

The angular distributions of the elastic and inelastic scattering of unpolarized 16 MeV protons by certain rare-earth isotopes were measured in ref. 10. Unfortunately, the measurements were confined to one inelastic-scattering channel (2^+), so that deformation parameters of order higher than the second could not be determined.

The inelastic scattering of protons by rare-earth nuclei and by actinides was investigated in Saclay.[11,12] The nuclear-deformation parameters of ^{232}Th and ^{238}U were determined for the first time from the scattering. These experimentally difficult studies are of interest because they have confirmed the existence of α-decay studies.[13-15]

The most systematic data on the hexadecapole-deformation parameters of nuclei in the rare-earth region were obtained in studies[16,17] of the scattering of α particles with energies close to 30 and 50 MeV. Sixth-order deformations were also estimated. The results of these studies were subsequently used to assess the aggregate of the experimental data on the deformations, in spite of certain doubts concerning the legitimacy of using an effective optical potential for complex particles. This pertains also to data on inelastic scattering of deuterons on rare-earth nuclei.[18-20]

In view of the recent increased tempo of work with accelerated heavy ions, the improvement of accelerators and sources of heavy ions, and also the technique of detection of γ radiation with the aid of germanium semiconductor detectors, many investigations of Coulomb excitation and of electromagnetic transitions in rare-earth nuclei have been reported. In addition to standard methods for measurement of the cross sections for excitation of low levels of nuclei by the Coulomb field of the incident charged particles,[21-24] measurements were made of the quadrupole moments of the excited states by the reorientation method.[25,26] The lifetimes of the excited states of nuclei were investigated by the method of the Doppler shift of the γ rays emitted as a result of Coulomb excitation.[27,28] Owing to the appreciable increase in the measurement accuracy, it was possible to obtain in these studies estimates of the hexadecapole-deformation parameters, and to verify, by measuring the reduced probabilities of the electromagnetic quadrupole transitions, the applicability of the rigid-axially-symmetrical-rotator model to a number of nuclei.[28] Indications were obtained[27] that the rigidity of the rotator is violated in the case of ^{152}Sm.

Thus, both inelastic scattering of charged particles and Coulomb excitation have by now become exact methods for obtaining spectroscopic nuclear data. After considering the main features of the experimental procedure, of the theoretical calculation methods, and of the comparison with the experiment, we discuss in the present article the spectroscopic information that can be obtained by investigating inelastic scattering, and compare this information with other data.

1. PRINCIPAL REQUIREMENTS ON THE EXPERIMENTAL PROCEDURE

Measurement of the angular distributions of inelastic scattering of charged particles by heavy nuclei is a difficult experimental task. This is due to the small difference between the energies of even the low-lying levels of even–even nuclei, and consequently the need of attaining a sufficient energy resolution in order to separate groups of charged particles scattered with excitation of closely lying levels. The excitation energy of the first rotational state amounts to 80-100 keV in the rare-earth region and 40-60 keV for actinides. It must also be rec-

ognized that the cross section for small-angle elastic scattering greatly exceeds the inelastic-scattering cross section. If the beam of the primary accelerated particles is not monochromatic enough, or if the scattered-particle detectors have poor resolution, an error is introduced not only in the measured inelastic-scattering cross section, but also in the elastic cross section.

The energy of the incident charged particles should not be less than the height of the Coulomb barrier, i.e., not less than 12-16 MeV for protons. Among the accelerators capable of providing charged particles of this energy, the best beam monochromaticity (about 2×10^{-4}) is possessed by tandem electrostatic generators. If cyclotrons are used, additional monochromatization of the beam is required as a rule. The use of beams from spectrometric cyclotrons, with large beam currents and approximate monochromaticity 10^{-4}, is quite promising.

As already noted, the use of a beam of polarized protons is of great importance for improvement of the accuracy of the analysis of the experimental data. The stringent requirements on the energy resolution of the proton beam when measurements are made of the elastic and inelastic scattering by heavy nuclei prevent the use of the secondary polarized-proton beam obtained after the primary beam is scattered by nuclei of targets having good polarizing ability. To obtain a sufficient secondary-beam intensity it is necessary to use thick targets, and this produces, as a result of the loss of energy in the target and of straggling, a considerable energy spread in the secondary beam also leads to a decrease in the experimental accuracy and to a lengthening of the measurement time.

The development of sources of polarized protons and deuterons, one of the most important attainments of modern experimental technique, makes it possible at present to measure the angular distributions of the asymmetry of scattering of polarized protons by all nuclei, including heavy ones. The degree of proton polarization obtained with such a source is close to unity.[29] Polarized-particle sources can be used in conjunction with a tandem accelerator or a cyclotron with external injection.[30]

The best results can be obtained with single-isotope targets in the form of free-standing foils. At the considered accelerated-ion energies, such foils (0.5-1 mg/cm^2) can be made from many isotopes of heavy nuclei. Frequently thinner targets, evaporated on carbon substrates, are used. Owing to the possible contamination of the target or its sputtering by the beam, it is desirable to perform the measurements simultaneously for all the investigated excited levels of the target nuclei and at several scattering angles. It is obvious that the last condition is not satisfied by magnetic charged-particle spectrometers, although they can have a resolution of approximately 10^{-4}, which is the best attainable with the presently available instruments. Indeed, the momentum analysis of particles is carried out in a limited range of values, and it is practically impossible to use them for the investigation of the excitation of many levels.

Magnetic spectrographs permit the analysis of scattered particles in a wide range of momenta, but it is difficult to make their resolving power better than 10^{-3} (refs. 31, 32). Magnetic spectrographs and magnetic spectrometers have a small aperture, and to obtain the total angular distribution of the elastically and inelastically scattered particles it is sometimes necessary to operate the apparatus for unrealistically long times.

The better surface-barrier semiconductor charged-particle detectors are those prepared by the lithium-drift method. They yield an approximate resolution $2 \cdot 10^{-3}$ at energies 10-20 MeV and can be used to study inelastic scattering with excitation of not-too-high levels of heavy nuclei. The aperture, which is limited only by the angular-resolution requirement, makes sufficiently rapid measurements possible. Use can be made of several detectors installed at different scattering angles. Recently many laboratories have made considerable progress in the development of semiconductor detectors with working-layer thickness of several millimeters, a thickness needed to detect the total-absorption pulse of charged particles of energy 10-30 MeV. When working with higher-energy particles it will apparently be preferable to use germanium in place of silicon.[33]

Attention should be called to the following shortcoming of semiconductor detectors as compared with magnetic analyzers: The distribution of the counts from a semiconductor detector, when a monochromatic particle beam is detected, is not symmetrical. The number of smaller-amplitude pulses is increased because of the temporary capture of the carriers by the traps,[34] and at higher energies, in addition, there may be an increase due to possible nuclear reactions in the detector material.[35] The asymmetry depends on the quality of the crystal. The region of lower-amplitude counts corresponds to higher levels excited in inelastic scattering. As a rule, these levels are excited with lower probability than the low-lying levels. For example, the excitation of each succeeding level of the rotational band 2^+, 4^+, 6^+ is smaller by approximately one order of magnitude than the preceding one. The aforementioned background of low-amplitude counts is a hindrance in the investigation of highly excited states.

The more stringent requirements with respect to monochromaticity of the beams and the energy resolution of the recording apparatus when measuring inelastic scattering from rare-earth nuclei give rise to large difficulties in the investigation of proton spin flip in inelastic scattering. These measurements consist of detecting the coincidences of the scattered protons with excitation of the 2^+ levels and the radiation from the decay of these states in a direction perpendicular to the scattering plane. In the case of heavy nuclei and at higher energies of the incident particles, the γ-radiation background is large and leads to an increase in the number of random coincidences. At the same time, at low energies of the 2^+ levels, the yield of γ radiation from the decay of these states decreases with increasing internal-conversion coefficient. Consequently, in addition to the requirement of a high energy resolution, it becomes necessary to use coincidence circuits with a high time resolution, on the order of several nanoseconds. The only known measurement of the spin-flip probability on deformed nuclei is in ref. 7.

The questions involved in the experimental proce-

dure used in our studies are considered in greater detail by Kurepin,[36] who discusses the interpretation and reduction of the spectra of pulses obtained from semiconductor detectors, and also the absolute normalization of the cross sections and the possible measurement errors.

Let us list the main requirements that must be satisfied in an experiment on inelastic scattering in order to obtain with sufficient accuracy the parameters of the theory. An energy two or three times higher than the Coulomb barrier is optimal for the incident charged particles. In the case of particles with spin, one can use beams of polarized ions and measure the angular distributions of the polarization and of the analyzing ability. It is desirable to obtain the angular distribution of inelastic scattering with excitation of a large number of states. For deformed even–even nuclei, a sufficient accuracy can be attained only by using data on the excitation of the rotational states 0^+, 2^+, 4^+, (6^+) of the band constructed on the ground state. The interval of the measured angles for elastic and inelastic scattering should be 30-170°, and it turns out that the calculations are more sensitive in the large-angle region.

At the present time, the aforementioned requirements can be satisfied in certain experimental investigations, and this will lead to the appearance of new studies of inelastic scattering of protons, deuterons, and α particles with excitation of collective states of heavy nuclei.

2. CALCULATION OF INELASTIC SCATTERING OF PROTONS BY THE METHOD OF COUPLING OF THE CHANNELS

In the theoretical reduction of the experimental data on inelastic scattering of protons by nuclei in the rare-earth region, attention must be called first to the appreciable cross sections for inelastic scattering with excitation of the lower levels of the nuclei, expecially in the case of strongly-deformed nuclei. The traditional methods of calculation in first-order perturbation theory no longer hold. A more accurate theory calls for allowance for the most essential inelastic-scattering channels when they are strongly coupled. We shall write down later a system of coupled equations for the scattering of nucleons by nuclei. We consider various methods of numerically solving this system. Particular attention will be paid to the justification and development of approximate calculation methods, such as allowance for second-order effects[37,38] and the method of successive approximation.[39] The approximate methods, which in certain cases yield results that agree with the exact calculation methods, are of great importance in the reduction of the experimental data. Indeed, the approximate methods result in considerable economy of computer time and therefore permit a larger number of calculations to be performed for a more accurate determination of the interaction parameters. As mentioned in the introduction, the low-lying excited states of heavy nuclei have clearly pronounced collective properties. Therefore, to describe the levels excited in inelastic scattering we use in this paper collective models, and treat the interaction of the incident particles with the nucleus in the form of a deformed optical potential. Since the form of the potential is not spelled out concretely in the sections devoted to methods of solving systems of coupled equations, these methods can be used also when attempts are made to describe microscopically the process of scattering with a realistic nucleon–nucleon potential.

Approximate methods that are faster from the point of view of computer time make it possible to perform calculations, within reasonable times, with complicated forms of interactions, allowance for which greatly complicates the problems. We consider below the influence of the diffuseness of the nuclear charge distribution, which must be taken into account at particle energies close to the Coulomb barrier. The introduction of a spin–orbit dependence into the optical potential makes it possible to calculate the polarization of the scattered particles, the analyzing ability, and also the probability of spin flip due to scattering.

System of Coupled Equations

We consider the scattering of nucleons by nuclei, such that the incident nucleon can experience, besides elastic scattering, also scattering with loss of energy and excite certain states of the target nucleus. Denoting by T the nucleon kinetic-energy operator, by V the operator of the interaction of the nucleon with the target nucleus, and by H_T the Hamiltonian of the target nucleus, we represent the total Hamiltonian of the system consisting of the nucleus and the nucleon interacting with it in the form

$$H = H_T + T + V. \tag{1}$$

We note that if it is necessary to take into account the internal structure of the incident particle, the Hamiltonian H_T can be broken up into two parts, corresponding to the internal structure of the nucleus and of the particle.

The wave functions χ_{IM} of the various states of the target nucleus, with spin I and projection M, are the eigenfunctions of the Hamiltonian H_T with energy eigenvalues ε:

$$H_T \chi_{IM} = \varepsilon_I \chi_{IM}. \tag{2}$$

The complete wave function Ψ of the system satisfies the following Schrödinger equation:

$$(H_T + T + V)\,\Psi = E\Psi, \tag{3}$$

where E is the total energy of the system.

The wave function Ψ can be represented in the form of an expansion in a complete system of wave functions $\mathcal{Y}^{JN}_{Ijl}$ of the different elastic- and inelastic-scattering channels with total angular momentum J and with projection N, corresponding to definite states of the target nucleus, nucleon orbital angular momenta l, and total nucleon angular momentum $\mathbf{j} = \mathbf{l} + \mathbf{s}$:

$$\Psi = \sum_{nI_nj_nl_nJ} f^{JN}_{nI_nj_nl_n}(r_n)\, \mathcal{Y}^{JN}_{I_nj_nl_n}. \tag{4}$$

This expansion, which is basic to the entire subsequent derivation of the system of coupled equations, con-

tains two important assumptions. First, it is assumed that regardless of the distance r_n between the nucleon and the nucleus in the channel n, the two particles do not lose their individuality and are described by certain specified wave functions. This assumption is valid for the two-particle problem or for scattering by a potential, but there would be little justification for using it to consider a many-particle problem. Second, the reaction channels are not included. These channels, however, are coupled quite weakly with the considered inelastic-scattering channels in the case of excitation of collective states in inelastic scattering. Both the vanishing of particles at short distances in the first approximation, and the absence of certain reaction channels in the second approximation are effectively taken into account subsequently by introducing the imaginary part of the optical potential.

The wave functions $\mathcal{Y}^{JN}_{Ijl}$ of the different inelastic-scattering channels can be represented as an expansion in the spin-angular functions of the incident nucleon Φ_{ljm_j} and the eigenfunctions χ_{IM} of the target nucleus:

$$\mathcal{Y}^{JN}_{Ijl} = \sum_{mjM} (IMjm_j \mid JN)\, \Phi_{ljm_j}\chi_{IM}, \tag{5}$$

where

$$\Phi_{ljm_j} = \sum_{m_l m_s} (lsm_l m_s \mid jm_j)\, Y_{lm_l}\chi_{sm_s}; \tag{6}$$

χ_{sm_s} are the spin wave functions of the nucleon.

Substituting (4) in (3), multiplying from the left by $\mathcal{Y}^{JN*}_{Ijl}$, and integrating over all the coordinates with the exception of the radial coordinate r, we obtain a system of coupled equations with respect to the radial functions $f^{JN}_{nIjl}(r)$:

$$[-T_r + (E-\varepsilon_i)]\, f^{JN}_{iIjl}(r) = \sum_{nI_njnln} \langle \mathcal{Y}^{JN}_{Ijl} \mid V \mid \mathcal{Y}^{JN}_{I_njnln}\rangle\, f^{JN}_{nI_njnln}(r), \tag{7}$$

where

$$T_r = -\frac{\hbar^2}{2\mu}\left(\frac{1}{r^2}\cdot\frac{d}{dr}\, r^2\, \frac{d}{dr} - \frac{l(l+1)}{r^2}\right).$$

In these equations, μ is the reduced mass; ε_i and ε_n are the energies of the states of the target nucleus in the inelastic-scattering channels i and n; E and $(E-\varepsilon_i)$ are the respective energies of the incident and outgoing nucleons. The energies are connected in the following manner with the wave numbers k_i and k_n in the channels i and n:

$$E = \varepsilon_i + \hbar^2 k_i^2/2\mu = \varepsilon_n + \hbar^2 k_n^2/2\mu. \tag{8}$$

If it is possible to separate the diagonal part of the interaction operator

$$V = V_{\text{diag}} + V_{\text{coup}}, \tag{9}$$

then the coupled equations take the form

$$[-T_r - V_{\text{diag}} + (E-\varepsilon_i)]\, f^{JN}_{iIjl}(r) = \sum_{nI_njnln} V^{J}_{I_njnln,\, Ijl}(r)\, f^{JN}_{nI_njnln}(r), \tag{10}$$

where an abbreviated notation is used for the matrix elements:

$$V^{J}_{I_njnln,\, Ijl} = \langle \mathcal{Y}^{JN}_{Ijl} \mid V_{\text{coup}} \mid \mathcal{Y}^{JN}_{I_njnln}\rangle. \tag{11}$$

Scheme for Exact Numerical Solution of the System of Coupled Equations

Assume that an exact numerical integration of the system of coupled equations (10) yielded certain radial wave functions $f^{JN}_{nI_njnln}$. Naturally, it is first necessary to reduce the infinite system of equations to a finite system. On the basis of physical considerations we can retain only the most essential strongly coupled inelastic-scattering channels.

The radial wave functions $f^{JN}_{nIjnln}(r)$ can then be used in (4) to construct the complete wave function. However, to calculate observable quantities such as the reaction cross section, the polarization, etc., the complete wave function must have a definite asymptotic form at large distances. We denote this complete wave function by Ψ^{+}_{α}. The plus sign means that, in accordance with the physical formulation of the problem, only converging waves are present in the input channel α, and in the remaining channels $n \neq \alpha$ there are only diverging waves. The wave function Ψ^{+}_{α} takes the following asymptotic form:

$$\Psi^{+}_{\alpha} \sim \chi_{I_\alpha M_\alpha}\chi_{sm_s}\exp(i\mathbf{k}_\alpha\mathbf{r}_\alpha) - \mu/(2\pi\hbar^2)\sum_n A_{n\alpha}(k_\alpha, k_n)\,\chi_{I_nM_n}\chi_{s'm_s'}\exp(ik_nr_n)/r_n, \tag{12}$$

where $A_{n\alpha}$ are elements of the scattering amplitude.

At a certain value of the radius R, which should be large enough, especially in the case when the Coulomb forces exert a strong influence, the total wave function (4) goes over into the function (12). It is then possible to determine the scattering-amplitude elements.

In the analysis of the scattering of charged particles it is meaningful, for convenience in calculation, to separate from the asymptotic value of the complete wave function the Coulomb part, i.e., the function that expresses the incident wave, and the wave scattered by the Coulomb field of the nucleus. It takes the form[40]

$$\Psi_{\text{Coul}} = \frac{1}{\sqrt{v_\alpha}}\frac{1}{k_\alpha}\sum_l i^l(2l+1)\exp(i\omega_{\alpha l})F_{\alpha l}/r_\alpha \times P_l(\cos\theta)\,\chi_{sm_s}\chi_{I_\alpha M_\alpha}, \tag{13}$$

where $F_{\alpha l}$ is the regular Coulomb function, $\omega_{\alpha l} = \sigma_{\alpha l} - \sigma_{\alpha 0}$ is the difference between the Coulomb phases, r_α is the radius vector in the input channel α, and v_α is the relative velocity in the channel α.

The asymptotic expression for the complete wave function for the scattering of charged particles by nuclei can then be expressed in the form

$$\Psi^{+}_{\alpha} = \Psi_{\text{Coul}}\delta_{n\alpha} + \sum_n \Psi_n, \tag{14}$$

or in expanded form

$$\Psi_\alpha^+ = \Psi_{\text{Coul}}\delta_{n\alpha} + i\frac{\sqrt{\pi}}{k_\alpha}\sum_{nJjlj_nl_n}\sqrt{2l_n+1}\times B^J_{nj_nl_n,\,\alpha jl}\frac{\exp i\{\rho_n-\eta_n\ln 2\rho_n+\sigma_{n0}\}}{\sqrt{v_n}\,r_n}\times(ls0m_{s'}\,|\,jm_s)\,(I_\alpha jM_\alpha m_s\,|\,JN)\,\mathcal{Y}^{JN}_{I_nj_nl_n}, \quad (15)$$

where $\rho_n = k_n r_n$ is the product of the wave number and the radius vector in the channel n; $\eta = Z_n Z_N e^2/(\hbar v_n)$ is the charge of the outgoing particle and of the nucleus in the channel n; v_n is the relative velocity in the channel n.

The coefficients $B^J_{njnl_n,\,\alpha jl}$ are connected with the corresponding scattering-matrix elements $U^J_{njnl_n,\,\alpha jl}$ (ref. 40):

$$B^J_{nj_nl_n,\,\alpha jl} = \exp(2i\omega_{nl})\,\delta_{n\alpha}\delta_{l_nl}\delta_{m_s'm_s}\delta_{mn0} - U^J_{nj_nl_n,\,\alpha jl}. \quad (16)$$

We consider now the basic principles of numerically determining the solutions[3,41] of the radial wave equations (10). The radial wave functions can be expressed in the form

$$f^{JN}_{nI_nj_nl_n}(r) = u^{JN}_{nI_nj_nl_n}(r)/r. \quad (17)$$

The system of coupled equations relative to the functions $u^{JN}_{nI_nj_nl_n}$ is accordingly changed into

$$\left[\frac{\hbar^2}{2\mu}\left(\frac{d^2}{dr^2}-\frac{l(l+1)}{r^2}\right)-V_{\text{diag}}+(E-\varepsilon_i)\right]u^{JN}_{iIjl}(r) = \sum_{nI_nj_nl_n}V^J_{I_nj_nl_n,\,Ijl}u^{JN}_{nI_nj_nl_n}(r). \quad (18)$$

It follows from (17) that the radial wave functions $U^{JN}_{nI_nj_nl_n}$ should vanish at the origin. One of the possible initial conditions that can be used for numerical solution of the system of coupled equations, at small values of r, is that all the radial wave functions vanish, with the exception of one function corresponding to a certain channel i. In this case the equation for the function $u^{JN}_{iIjl}(r) \equiv u_i(r)$ from among the equations of the system (18) near the origin recalls the equation for the scattering by a square-well potential. Then the function near the origin can be approximated by a spherical Bessel function.

Taking into account the behavior of the spherical Bessel function as $r \to 0$, we write

$$\lim_{r\to 0} u_i^{(p)}(r) = \begin{cases} \frac{(kr)^{l+1}}{(2l+1)!!}; & p = i; \\ 0; & p \neq i. \end{cases} \quad (19)$$

The numerical integration of the radial Schrödinger equations for each of the partial waves can then be carried out with the aid of one of the methods proposed in ref. 42 (Runge–Kutta, Cowell, or Numerov). As the result, we can obtain N radial wave functions corresponding to N coupled equations. Since no conditions on the behavior of the radial wave functions at large distances are imposed on the integration, the resultant solutions contain both outgoing and scattered waves. However, as seen from the asymptotic form of the wave function (12), only the solution corresponding to the input channel can contain incident and scattered waves, whereas the solutions corresponding to the other channels contain only scattered waves.

To construct the complete wave function with the required asymptotic form one can modify the initial conditions (19), specifying in turn the radial functions of each of the N channels in the form of a series expansion. Thus, the superscript p in Eq. (19) runs through the values from 1 to N. In accordance with the N different initial conditions we obtain N different solutions, each of which contains N radial functions. We represent the radial functions for each of the channels in the form of a linear combination of the obtained solutions. Then, equating their values as well as the values of the derivatives at the radius R at which the functions are matched to the asymptotic value of the wave function in each channel, we obtain a system of 2N linear algebraic equations with respect to N coefficients of linear combination a_i and N coefficients $B^J_{njnl_n,\,\alpha jl}$ which enter in the relation (15):

$$\begin{aligned}
&a_1u_1^{(1)} + a_2u_1^{(2)} + \ldots + a_Nu_1^{(N)} = \Psi_1 + \Psi_{\text{Coul}};\\
&a_1u_2^{(1)} + a_2u_2^{(2)} + \ldots + a_Nu_2^{(N)} = \Psi_2;\\
&\cdots\cdots\cdots\cdots\cdots\cdots\\
&a_1u_N^{(1)} + a_2u_N^{(2)} + \ldots + a_Nu_N^{(N)} = \Psi_N;\\
&a_1u_1^{(1)\prime} + a_2u_1^{(2)\prime} + \ldots + a_Nu_1^{(N)\prime} = \Psi_1' + \Psi_{\text{Coul}}';\\
&\cdots\cdots\cdots\cdots\cdots\cdots\\
&a_1u_N^{(1)\prime} + a_2u_N^{(2)\prime} + \ldots + a_Nu_N^{(N)\prime} = \Psi_N'.
\end{aligned} \quad (20)$$

We can thus find the coefficients $B^J_{njnl_n,\,\alpha jl}$. The scattering amplitude is expressed in terms of these coefficients in the following manner:

$$A_{nm_s'M_n,\,\alpha m_sM_\alpha} = \frac{2\pi\hbar^2}{\mu}\sqrt{\frac{v_\alpha}{v_n}}\left\{f_c(\theta)\,\delta_{n\alpha}\delta_{m_s'm_s}\delta_{M_nM_\alpha} + i\frac{\sqrt{\pi}}{k_\alpha}\sum_{JNjlj_nl_nm_nm_{j_n}}\sqrt{2l_n+1}\,(ls0m_s\,|\,jm_j)\times(jI_\alpha m_jM_\alpha\,|\,JN)\,(l_ns'm_nm_s'\,|\,j_nm_{j_n})\times(j_nI_nm_{j_n}M_n\,|\,JN)\,Y_{l_nm_n}(\theta,\varphi)\,B^J_{nj_nl_n,\,\alpha jl}\right\}. \quad (21)$$

The primed quantities (s', m'_s) and the unprimed ones denote the nucleon spin and spin projection after and before scattering, respectively.

The Coulomb-scattering amplitude in Eq. (21) takes the usual form:

$$f_c(\theta) = -\frac{ZZ\,e^2}{2\mu v_\alpha^2}\operatorname{cosec}^2\frac{\theta}{2}\exp(-2i\eta_\alpha\ln\sin\theta/2). \quad (22)$$

The notation of this equation is analogous to that used in Eq. (15).

Expressions for the elastic- and inelastic-scattering cross sections, the polarization, the analyzing ability, and the nucleon spin-flip probability in terms of the scattering amplitude will be written out after we discuss the approximate methods of solving the system of coupled equations.

Solution of System of Coupled Equations by the Method of Successive Approximations

To distinguish clearly between the different stages of the successive approximations when solving a system of coupled equations, we express the system of differential equations (10) in the form of a system of integral equations. To this end we introduce for each scattering channel the Green's function $G_n(r, r')$:

$$[-T_r - V_{nn} + (E - \varepsilon_n)]\, G_n(r, r') = \delta(r - r'). \tag{23}$$

For the diagonal matrix elements in the n-th channel we use here the symbol V_{nn}.

To construct the integral equations we need also radial wave functions $g^{JN}_{nl_n j_n l_n}$ that satisfy homogeneous equations of the type (10). To simplfy the notation, we omit the angular-momentum labels, which are of no importance in the general analysis, and assume that they are incorporated in the channel label n. The homogeneous equations take the form

$$[-T_r - V_{nn} + (E - \varepsilon_n)]\, g_n(r) = 0. \tag{24}$$

In the subsequent expressions, again for simplicity, we shall write down the radial wave functions of Eqs. (10) in the form $f_n(r)$, the wave functions of the complete system of functions $\mathcal{Y}_n$, and the matrix elements

$$\langle \mathcal{Y}_n | V_{\text{coup}} | \mathcal{Y}_k \rangle = V_{nk}. \tag{25}$$

With the aid of (23) and (24) we can write down an expression for the radial wave functions of each channel:

$$f_n(r) = g_n(r)\, \delta_{n\alpha} + \int (dr')\, G_n(r, r') \sum_k V_{nk} f_k(r'). \tag{26}$$

Equations (26) thus constitute a system of coupled integral equations for the problem in question. The wave functions $g_n(r)$ in this system can be easily obtained, since they are solutions of the uncoupled equations (24). If an optical potential is used for the interaction, then the functions $g_n(r)$ are usually called distorted waves.

If the Green's functions $G_n(r, r')$ are suitably chosen,[43] we can obtain the solutions of the system (26) and from these solutions, according to (4), we can obtain the complete wave function Ψ^+_α, which has the required asymptotic properties (12). The concrete form of the usually employed Green's functions will be given below when we deal with the calculation of the inelastic-scattering cross sections.

An expression for the scattering amplitude from the input channel α to a certain inelastic-scattering channel γ follows from the formal scattering theory[44] and is called the Gell-Mann and Goldberger relation for scattering by two potentials:

$$A_{\gamma\alpha} = A_0 \delta_{\gamma\alpha} + \langle \mathcal{Y}_\gamma g^-_\gamma | V_{\text{coup}} | \Psi^+_\alpha \rangle. \tag{27}$$

The scattering-amplitude element A_0 is governed by a separated diagonal part of the potential (9). Since the latter cannot lead to excitation of the target-nucleus states or to reactions, the scattering amplitude A_0 contributes only to the elastic scattering. The minus sign of the wave function g^-_γ denotes that it is necessary to choose from among the solutions of the corresponding equation (24) only those containing converging waves.

One can attempt to obtain solutions of the integral equations (26), under the condition that the number of coupled channels is limited, on the basis of physical considerations by following in principle the Tamm–Dancoff method.[45] For the inelastic-scattering problem, this method of successive approximations was formulated in final form by Reynal,[39] although the first iterations were used earlier for some specific problems.[37,46]

Following Reynal,[39] we shall designate the radial wave functions entering in the system (26) by two indices: The lower denotes the number of the channel and the upper the order of the iteration. The matrix elements are written in the notation of (25). Just as in the Tamm–Dancoff method, in each successive step, i.e., in each calculation of the function of the next channel and the next iteration, we use the quantities obtained during the preceding stage.

In the zeroth approximation, we take as the input-channel function the solution of Eq. (24) for the input channel, neglecting the presence of other inelastic-scattering channels:

$$f_0^{(0)}(r) = g_0(r); \quad f_i^{(0)} = 0, \quad i \neq 0. \tag{28}$$

Obviously, the zeroth approximation corresponds to the elastic-scattering problem. Methods for solving this problem with the use of an optical potential are extensively explained in the literature[42] and will not be considered further.

In the first-order approximation of the method, we consider first the wave function of a certain inelastic-scattering channel and call it the first channel. We use this in the appropriate equation from (26):

$$f_1^{(1)}(r) = \int G_1(r, r')\, V_{10}(r')\, f_0^{(0)}(r')\, dr'. \tag{29}$$

When writing down the wave function of the second inelastic-scattering channel in accordance with Eq. (26), we take into account the presence of the wave function of the first channel (29):

$$f_2^{(1)}(r) = \int G_2(r, r')\, [V_{20}(r')\, f_0^{(0)}(r') + V_{21}(r')\, f_1^{(1)}(r')]\, dr'. \tag{30}$$

In the absence of other inelastic-scattering channels, the wave function corresponding to each channel in the first-order approximation is expressed in the form

$$f_0^{(1)}(r) = g_0(r) + \int G_0(r, r')\, [V_{01}(r')\, f_1^{(1)}(r') + V_{02}(r')\, f_2^{(1)}(r')]\, dr'. \tag{31}$$

In the presence of N inelastic-scattering channels, relations (30) and (31) can be easily generalized to

$$f_i^{(1)}(r)=\int G_i(r,r')\Big[V_{i0}(r')\,f_0^{(0)}(r')+\sum_{j=1}^{i-1}V_{ij}(r')\,f_j^{(1)}(r')\Big]dr'; \quad (32)$$

$$f_0^{(1)}(r)=g_0(r)+\int G_0(r,r')\sum_{j=1}^{N}V_{0j}(r')\,f_j^{(1)}(r')\,dr'. \quad (33)$$

The wave functions of the inelastic-scattering channels and of the input channel, calculated in the n-th order of iteration, are expressed by the following relations:

$$f_i^{(n)}(r)=\int G_i(r,r')\Big[V_{i0}(r')\,f_0^{(n-1)}(r')+\sum_{j=1}^{i-1}V_{ij}(r')\,f_j^{(n)}(r')+\sum_{j=i+1}^{N}V_{ij}(r')\,f_j^{(n-1)}(r')\Big]dr'; \quad (34)$$

$$f_0^{(n)}(r)=g_0(r)+\int G_0(r,r')\sum_{j=1}^{N}V_{0j}(r')\,f_j^{(n)}(r')\,dr'. \quad (35)$$

The convergence and rate of convergence of the successive-approximation method, just as of the Tamm–Dancoff method, can be investigated only when solving a concrete problem. Since we use in each successive iteration the wave functions calculated during the preceding stage, an important role in the convergence of the method is played by the optimal sequence with which the successive channels are chosen. The inelastic-scattering channel following the input channel should be the one to the nuclear level with the strongest coupling to the ground state of the nucleus.

Calculation Method With Allowance for Only One Inelastic-Scattering Channel

Sometimes in the course of an experiment on inelastic scattering it turns out that only one inelastic-scattering channel is significant, i.e., the inelastic-scattering cross section in the other channels is negligibly small. If it turns out at the same time that the cross section for inelastic scattering with excitation of this level is small in comparison with the elastic-scattering cross section, then it can be assumed that the complete wave function Ψ consists mainly of the part corresponding to the input channel of the elastic scattering.[47] This assumption is justified in a region outside the range of action of the nuclear forces. To perform numerical calculations and to integrate over all of space, it is necessary to assume that the wave function Ψ includes only the input channel at all distances. This is the main assumption of the method. Designating the input channel by the subscript zero, we obtain in place of relation (4)

$$\Psi\approx\sum_{j_0l_0J}f^{JN}_{0I_0j_0l_0}(r)\,\mathcal{Y}^{JN}_{I_0j_0l_0}. \quad (36)$$

The system of coupled equations (10) is transformed into two independent equations for each value of the total angular momentum:

$$[-T_{r0}-V_{00}+(E-\varepsilon_0)]\,f^{JN}_{0I_0j_0l_0}\approx 0; \quad (37)$$

$$[-T_{r1}-V_{11}+(E-\varepsilon_1)]\,f^{JN}_{1I_1j_1l_1}=\sum_{l_0j_0}V^{J}_{I_1j_1l_1,\,I_0j_0l_0}f^{JN}_{0I_0j_0l_0}, \quad (38)$$

where

$$T_{rl}=-\frac{\hbar^2}{2\mu}\left(\frac{1}{r^2}\cdot\frac{d}{dr}r^2\frac{d}{dr}-\frac{l_i(l_i+1)}{r^2}\right);$$

V_{00} and V_{11} are the corresponding diagonal elements of the interaction in channels zero and one. Obviously, these equations can be solved in succession. The first equation coincides with Eq. (24) for the distorted waves. We write also the homogeneous equation for finding the distorted waves $g^{JN}_{1I_1j_1l_1}$ in the inelastic-scattering channel:

$$[-T_{r1}-V_{11}+(E-\varepsilon_1)]\,g^{JN}_{1I_1j_1l_1}=0. \quad (39)$$

Then, within the framework of the considered method, the scattering amplitude can be calculated directly. From (27), (36), and (11) it follows that

$$A_{10}^{(I)}=\sum_{JNj_1l_1}\langle\mathcal{Y}^{JN}_{I_1j_1l_1}g^{JN}_{1I_1j_1l_1}|\,V_{\text{coup}}|\,\Psi\rangle \approx\sum_{JNj_1l_1j_0l_0}\int g^{JN}_{1I_1j_1l_1}V^{J}_{I_1j_1l_1,\,I_0j_0l_0}f^{JN}_{0I_0j_0l_0}r^2\,dr. \quad (40)$$

The last relation coincides with the amplitude of the DWBA method, obtained in the first-order Born approximation with distorted waves.[46]

Thus, to use the method with only one inelastic-scattering channel taken into account, it is necessary that the elastic process prevail over the inelastic one, but there be no coupling between the chosen inelastic-scattering channel and the other inelastic-scattering channels, i.e., that the corresponding matrix elements (11) be small. In spite of the use of the assumption (36), for which there is little theoretical justification, this method was used successfully for calculations mainly for light and medium nuclei. When the foregoing applicability conditions are satisfied, a more exact allowance for the channel coupling yields, as a rule, a small correction to the cross sections calculated by this method.

Allowance for Second-Order Effects in the Presence of Two Inelastic-Scattering Channels

We consider here a calculation method[37,38] for a case frequently encountered in experiment, when in addition to the elastic-scattering channel there is a first inelastic-scattering channel coupled with the elastic channel, and the cross section for inelastic scattering with excitation of this level constitutes a small fraction of the elastic-scattering cross section. In addition, there is a second inelastic-scattering channel, coupled mainly with the first inelastic-scattering channel. Let also the cross section for excitation of the second level be much smaller than the excitation cross section of the first level. If we are interested just in the calculation of the cross section for

elastic scattering with excitation of the second level, then it is obvious that the method considered above will not do. Indeed, in addition to the direct excitation of this level, a significant and even decisive role may be played by a two-step process that proceeds via excitation of the first level coupled with the ground state. By way of example we can cite the scattering of nucleons by deformed nuclei at large values of the deformation, with excitation of the levels 0^+, 2^+, and 4^+ of the ground-state rotational band.

Under the physical assumptions made above, it is natural to assume that the complete wave function Ψ consists mainly of terms corresponding to the input channel and the first inelastic-scattering channel:

$$\Psi \approx \sum_{j_0 l_0 J} f^{JN}_{0 I_0 j_0 l_0}(r)\, \mathcal{Y}^{JN}_{I_0 j_0 l_0} + \sum_{j_1 l_1 J} f^{JN}_{1 I_1 j_1 l_1}(r)\, \mathcal{Y}^{JN}_{I_1 j_1 l_1}. \qquad (41)$$

However, by virtue of the predominance of the elastic process over all the inelastic processes, we neglect also the second term in the sum (41) when we write down an equation of the type (10) for the input channel. The system of coupled equations (10) then takes the form of the following three groups of equations for each value of the total angular momentum:

$$[-T_{r0} - V_{00} + (E-\varepsilon_0)]\, f^{JN}_{0 I_0 j_0 l_0} \approx 0; \qquad (42)$$

$$[-T_{r1} - V_{11} + (E-\varepsilon_1)]\, f^{JN}_{1 I_1 j_1 l_1} \approx \sum_{l_0 j_0} V^{J}_{I_1 j_1 l_1,\, I_0 j_0 l_0} f^{JN}_{0 I_0 j_0 l_0}; \qquad (43)$$

$$[-T_{r2} - V_{22} + (E-\varepsilon_2)]\, f^{JN}_{2 I_2 j_2 l_2} = \sum_{l_0 j_0} V^{J}_{I_2 j_2 l_2,\, I_0 j_0 l_0} f^{JN}_{0 I_0 j_0 l_0} + \sum_{l_1 j_1} V^{J}_{I_2 j_2 l_2,\, I_1 j_1 l_1} f^{JN}_{1 I_1 j_1 l_1}. \qquad (44)$$

We see that Eq. (42) coincides with (37). This means that in both the considered methods, which are based on perturbation theory, distorted waves are used as the radial wave functions of the input channel.

Equation (43) coincides only outwardly with (38). In the case of two inelastic-scattering channels, the equation for finding the radial wave function of the first inelastic-scattering channel becomes approximate because the term responsible for the coupling of this channel with the second inelastic-scattering channel is discarded. This is the gist of the basic principle of the proposed generalized Born approximation,[37,38] when all the couplings are neglected except the lower-order couplings responsible for the observed excitation of the nuclear levels.

It is here that the similarity of this calculation method to the successive-approximations method considered above manifests itself. In the successive-approximations method one also includes in the calculation, in succession, new inelastic-scattering channels. However, after several iterations it is possible to obtain convergence and by the same token take into account the initially discarded couplings. On the other hand the calculation in the generalized Born approximation is limited beforehand by the considered problem with the assumptions made concerning the relative couplings between the channels.

From the point of view of the performance of the calculations, the method considered here for taking the second-order effect into account is close to the first order of the successive-approximations method. Relations (29) and (30) are respectively integral forms of (43) and (44). The only difference is that the input-channel wave function (31) is calculated more accurately.

To find the inelastic-scattering amplitudes it is not necessary to solve Eq. (44) with respect to $f^{JN}_{2 I_2 j_2 l_2}$, but it is necessary to know for both the first and second inelastic-scattering channels the distorted waves $g^{JN}_{1 I_1 j_1 l_1}$ and $g^{JN}_{2 I_2 j_2 l_2}$ satisfying equations analogous to (39).

The wave function of the first inelastic-scattering channel will be expressed in terms of the corresponding Green's function in accordance with the relation (26):

$$f^{JN}_{1 I_1 j_1 l_1}(r) = \int G_{1 I_1 l_1}(r, r') \sum_{l_0 j_0} V^{J}_{I_1 j_1 l_1,\, I_0 j_0 l_0} f^{JN}_{0 I_0 j_0 l_0}(r')^2\, dr'. \qquad (45)$$

Then, using (27) and the introduced approximation (41) relative to the complete wave function, we can obtain the expressions for the scattering amplitudes.

For the sake of brevity we write down first the expressions for the scattering amplitudes A_{10} of the first channel, A_{20} of the second channel, and A_{00} of the elastic-scattering channel, in the symbolic form

$$A_{10} \approx \langle \mathcal{Y}_1 g_1(r) \,|\, V_{\text{coup}} \,|\, [\mathcal{Y}_0 f_0(r) + \mathcal{Y}_1 \int G_1(r, r')\, V_{10} f_0(r')\, (dr')] \rangle; \qquad (46)$$

$$A_{20} \approx \langle \mathcal{Y}_2 g_2(r) \,|\, V_{\text{coup}} \,|\, [\mathcal{Y}_0 f_0(r) + \mathcal{Y}_1 \int G_1(r, r')\, V_{10} f_0(r')\, (dr')] \rangle; \qquad (47)$$

$$A_{00} \approx A_0 + \langle \mathcal{Y}_0 f_0(r) \,|\, V_{\text{coup}} \,|\, [\mathcal{Y}_1 \int G_1(r, r')\, V_{10} f_0(r')\, (dr')] \rangle. \qquad (48)$$

It follows from (46) and (47) that the inelastic-scattering amplitudes can be represented in the form of a sum of two amplitudes. The first term of the sum corresponds to the scattering amplitude in first-order DWBA and takes the form (40). The second term of the sum expresses the scattering amplitudes in the second-order DWBA and takes into account multiple, in this case two-fold, excitation. For the amplitude A_{20}, the two-fold excitation process proceeds via an intermediate first level of the nucleus. For the amplitude A_{10} this is rescattering at the first level.

We present a more detailed relation for the scattering amplitude $A_{20}^{(II)}$, which expresses the contribution of the second-order effects when the second level is excited in inelastic scattering, in the second order of the Born approximation:

$$A^{(II)}_{20} = \sum_{\substack{JN j_2 l_2 j_0 l_0 \\ I_1 j_1 l_1}} \int (r^2\, dr)\, g^{JN}_{2 I_2 j_2 l_2} V_{I_2 j_2 l_2,\, I_1 j_1 l_1} \int G_{I_1 l_1} V_{I_1 j_1 l_1,\, I_0 j_0 l_0} \times f^{JN}_{0 I_0 j_0 l_0}(r')^2\, dr'. \qquad (49)$$

We note that the second-order cross section may exceed the first-order cross section for a definite relation between the matrix elements $V_{I_2 j_2 l_2, I_0 j_0 l_0}$ responsible for the direct excitation of this level and the elements $V_{I_2 j_2 l_2, I_1 j_1 l_1}$ and $V_{I_1 j_1 l_1, I_0 j_0 l_0}$ responsible for the multiple excitation.

The main term in expression (48) for the elastic-scattering amplitude is A_0, the amplitude of the elastic scattering due to only the diagonal part of the interaction. When this interaction is approximated by an optical potential, say in the Woods–Saxon form,[48] the calculation of the amplitude A_0 coincides fully with the calculation of the elastic-scattering amplitude in the usual optical model.[42,49] The expression for this amplitude can be easily obtained as a particular case of expression (21). The coefficients B_l^J can be determined from (16) with the aid of the scattering matrix elements or the scattering phase shifts. As seen from (15), these coefficients enter also in the asymptotic expression for the wave function. After numerically solving the radial wave equation (42) for the elastic-scattering channel, the solution obtained must be matched, at a certain matching radius R outside the range of action of the nuclear potential, to the asymptotic value of the radial wave function:

$$\varphi_l^J(R) = F_l(\eta, kR) + B_l^J\,[G_l(\eta, kR) + iF_l(\eta, kR)], \tag{50}$$

where F_l and G_l are the regular and irregular Coulomb wave functions. We can then find the coefficients B_l^J, and consequently also the elastic-scattering amplitude A_0.

The second term in (48) is the second-order amplitude. The appearance of this amplitude is due to the virtual excitation of the first states of the target nucleus. As will be seen below, when numerical calculations are considered, the second-order amplitude makes an appreciable contribution to the elastic-scattering cross section even in the case of not very strong coupling between the first inelastic-scattering channel and the input channel.

We emphasize once more, in conclusion, that with increasing channel coupling the method may become useless. It is then necessary to obtain an exact solution of the problem or to perform a number of iterations in the successive-approximation method.

Calculation of the Scattering Amplitudes in the Second Order of the Distorted-Wave Born Approximation

To carry out concrete calculations of the second-order amplitudes, which are given by (49), it is necessary to know the Green's functions G_{Il}. It is obvious that the Green's function should determine with the aid of (41) and (45) a complete wave function having the asymptotic properties (12) specified by the conditions of the problem. The construction of the Green's function of the radial Schrödinger wave equation was considered in refs. 50 and 51. It was shown that this function can be expressed in terms of certain solutions of a homogeneous radial Schrödinger equation

$$G_{Il}(r, r') = (2\mu k/\hbar^2 i)\, g_l(kr_<)\, y_l(kr_>), \tag{51}$$

where $r_>$ and $r_<$ are respectively the larger and smaller of the values r and r'; $g_l(kr)$ is the previously introduced regular solution of the homogeneous Schrödinger equation (42), having an asymptotic form

$$g_l(kr) \sim (1/kr)\sin(kr - \eta\ln 2kr - l\pi/2 + \sigma_l); \tag{52}$$

$y_l(kr)$ is the irregular solution of the same equation, with an asymptotic form

$$\left.\begin{aligned} &y_l(kr) \sim [1/(i\,kr)]\exp[i\,(kr - \eta\ln 2kr - l\pi/2 + \sigma_l)];\\ &\sigma_l = \arg[\Gamma(l+1+i\eta)]. \end{aligned}\right\} \tag{53}$$

In analogy with the calculations by the usual optical model, these solutions can be matched, after numerically solving the Schrödinger equation, at a certain distance outside the effective range of the nuclear forces, to a linear combination of Coulomb wave functions in the form (50). We write down the expression for the Wronskian of these functions:

$$W(g, y) = y(dg/dr) - g(dy/dr) = k. \tag{54}$$

The expressions for the scattering amplitudes are obtained after constructing the complete wave function (41) with the aid of the Green's function and after comparing it with the asymptotic behavior (12). The proton spin is not taken into account in the equations presented. It is relatively easy to introduce the proton spin into the equations if necessary.

The first-order scattering amplitude is

$$\begin{aligned} A_{20}^{(I)} = (4\pi)^{3/2} &\sum_{Jl_1l_2m_2} \exp[i\,(\sigma_{l_0} + \sigma_{l_2})]\, Y_{l_2m_2}(\theta, \varphi)\\ &\times \sqrt{2l_0+1}\,(I_2l_2M_2m_2\,|\,JM_0)\\ &\times (I_0l_0M_00\,|\,JM_0)\int_0^\infty r^2\,dr\,g_{l_2}V^J_{I_2l_2,\,I_0l_0}g_{l_0}. \end{aligned} \tag{55}$$

The second-order scattering amplitude determines a two-step process proceeding via excitation of the intermediate state I_1l_1:

$$\begin{aligned} A_{20}^{(II)} = (4\pi)^{3/2} &\sum_{JI_1l_2l_1l_0m_2} \exp[i\,(\sigma_{l_0} + \sigma_{l_2})]\, Y_{l_2m_2}(\theta, \varphi)\\ &\times \sqrt{2l_0+1}\,(I_2l_2M_2m_2\,|\,JM_0)\,(I_0M_0l_00\,|\,JM_0)\\ &\times \Big\{\int_0^\infty r^2\,dr\,g_{l_2}V^J_{I_2l_2,\,I_1l_1}y_{l_1}\int_0^r g_{l_1}V^J_{I_1l_1,\,I_0l_0}\,g_{l_0}\,(r')^2\,dr'\\ &+\int_0^\infty r^2\,dr\,g_{l_2}V^J_{I_2l_2,\,I_1l_1}\,g_{l_1}\int_r^\infty y_{l_1}V^J_{I_1l_1,\,I_0l_0}\,g_{l_0}\,(r')^2\,dr'\Big\}. \end{aligned} \tag{56}$$

The appearance of irregular solutions y_l in the double integrals of (56) is most inconvenient for numerical calculations, and doubts may be raised concerning the stability of the numerical values.

It turns out, however, that the irregular solutions can be completely eliminated from the integrands. To this end we introduce new regular and irregular functions α_l and β_l:

$$rg_l(kr) \equiv \alpha_l(kr); \quad ry_l(kr) \equiv \beta_l(kr). \tag{57}$$

Then the radial integrals of (56) take the form

$$\mathcal{J} = \int_0^{r_{max}} dr\alpha_{l_2} V^J_{l_2 l_1} \beta_{l_1} \int_0^r dr' \alpha_{l_1} V^J_{l_1 l_0} \alpha_{l_0}$$
$$+ \int_0^{r_{max}} dr\alpha_{l_2} V^J_{l_2 l_1} \alpha_{l_1} \int_r^{r_{max}} dr' \beta_{l_1} V^J_{l_1 l_0} \alpha_{l_0}, \quad (58)$$

where r_{max} should be chosen such that $V^J(r_{max}) \approx 0$. For a pure nuclear interaction, this condition can be easily attained. When the Coulomb interaction is taken into account, r_{max} should be chosen near 20–40 F, depending on the Coulomb contribution to the double-excitation process.

Using the expression for the Wronskian $W(\alpha, \beta)$, we obtain

$$d(\beta/\alpha)/dr = (1/\alpha^2)[\alpha(d\beta/dr) - \beta(d\alpha/dr)] = -k/\alpha^2. \quad (59)$$

Substituting this value in (58) and integrating by parts twice, we rewrite (58) in the form

$$\mathcal{J} = \frac{\beta_{l_1}(r_{max})}{\alpha_{l_1}(r_{max})} \int_0^{r_{max}} dr\alpha_{l_2} V^J_{l_2 l_1} \alpha_{l_1} \int_0^{r_{max}} dr\alpha_{l_1} V^J_{l_1 l_0} \alpha_{l_0} + \frac{1}{ik}$$
$$\times \int_0^{r_{max}} \frac{dr}{\alpha^2_{l_1}} \left(\int_0^r dr' \alpha_{l_2} V^J_{l_2 l_1} \alpha_{l_1} \right) \left(\int_0^r dr' \alpha_{l_1} V^J_{l_1 l_0} \alpha_{l_0} \right). \quad (60)$$

Thus, in the calculation of the second-order amplitude one uses integrals of the type $\int_0 dr \alpha_l V^J_{l l''} \alpha_{l'}$, which are analogous to those entering in the expression for the first-order amplitude (55). The irregular solution must be calculated only in the asymptotic region. A similar elimination of irregular solutions in perturbation theory in the general case was considered in ref. 51. In view of the singularity of the irregular solutions at r = 0, the necessary condition for the integration by parts is the rapid vanishing of $V^J(r)$ as $r \to 0$.

Successive-Approximations Method in the Differential-Equations Representation

If we continue to introduce new inelastic-scattering channels, then the number of successively solved equation of the type (42)–(44) increases. Introducing additionally a relation much more accurate than (42) for the input scattering channel, we obtain the first iteration of the successive-approximations method. We present the calculation sequence proposed by Reynal.[39] We use in the equations the abbreviated notation introduced above. Then the considered system of coupled equations (10) takes the form

$$[-T_r - V_{ii} + (E - \varepsilon_i)] f_i(r) = \sum_j V_{ji}(r) f_j(r). \quad (61)$$

In the zeroth order, only the input elastic-scattering channel is considered. Then the only wave function that differs from zero is $f_0^{(0)}(r) = g_0(r)$. As before, we denote by $g_i(r)$ the solutions of the homogeneous equations corresponding to (61).

In first order we first consider an equation of the type (43):

$$[-T_r - V_{11} + (E - \varepsilon_1)] f_1^{(1)}(r) = V_{10}(r) f_0^{(0)}(r). \quad (62)$$

As shown in ref. 39, it is possible to find a certain numerical solution $\varphi_1(r)$ of this equation, and construct the solution $f_1^{(1)}(r) = \varphi_1(r) + \alpha g_1(r)$, where α is determined by matching to the asymptotic wave function $G_l(r) + iF_l(r)$. Equations of the type (62) are analogously solved for other channels, each time with allowance for the previously obtained solutions $f_j^{(1)}(r)$. The first iteration is completed by solving the equation for the determination of the input-channel wave function:

$$[-T_r - V_{00} + (E - \varepsilon_0)] f_0^{(1)}(r) = \sum_{j>0} V_{j0}(r) f_j^{(1)}(r). \quad (63)$$

The solution is of the form $f_0^{(1)}(r) = \varphi_0(r) + \alpha g_0(r)$, where α can be obtained by matching to the asymptotic relation (50).

In the calculation of the higher orders of the iteration one uses all the wave functions obtained during the preceding stages:

$$[-T_r - V_{ii} + (E - \varepsilon_i)] f_i^{(n)}(r) = V_{0i}(r) f_0^{(n-1)}(r)$$
$$+ \sum_{0<j<i} V_{ji}(r) f_j^{(n)}(r) + \sum_{j>i} V_{ji}(r) f_j^{(n-1)}(r). \quad (64)$$

Expression for the Cross Sections, the Polarization, Analyzing Ability, and the Spin-Flip Probability in Terms of the Scattering Amplitude

After calculating the scattering amplitudes (21) with the aid of the exact or approximate methods, all the experimentally observed quantities can be expressed in terms of these amplitudes. In the experiments described in the present paper, these are the differential scattering cross sections, the angular dependences of the polarization, of the asymmetry, and of the analyzing ability and the spin-flip probabilities. We write down the necessary relations (see also ref. 52).

To simplify the notation, we introduce scattering amplitudes that differ from (21) by a numerical coefficient:

$$F_{nm'_s M_n, 0 m_s M_0} = [\mu/(2\pi\hbar^2)] \sqrt{k_n/k_0}\, A^J_{nm'_s M_n, 0 m_s M_0}. \quad (65)$$

Inasmuch as the projections m'_s and m_s assume values $\pm 1/2$ for proton scattering, and designating these values only by the symbols $\pm$, we represent the scattering amplitude in matrix form:

$$F^{M_n M_0} = \begin{pmatrix} F^{M_n M_0}_{++} & F^{M_n M_0}_{+-} \\ F^{M_n M_0}_{-+} & F^{M_n M_0}_{--} \end{pmatrix}. \quad (66)$$

We do not distinguish here between the elastic- and inelastic-scattering channels, since this distinction is contained only in the notation for the scattering amplitude.

The elements of this matrix are not independent. On the basis of the general symmetry property of the scattering amplitude, which is equivalent to the Bohr theorem[53]

$$F_{-m_s', -M_n, -m_s, -M_0} = (-1)^{m_s - m_s' - M_n + M_0} F_{m_s' M_n m_s M_0}, \quad (67)$$

we obtain

$$F_{++}^{M_n M_0} = (-1)^{M_0 - M_n} F_{--}^{-M_n, -M_0};$$
$$F_{+-}^{M_n M_0} = -(-1)^{M_0 - M_n} F_{-+}^{-M_n, -M_0}. \quad (68)$$

The expression for the cross section then takes the form

$$\frac{d\sigma}{d\Omega}(\theta) = \frac{2}{(2s+1)(2I_0+1)} \sum_{M_n M_0} (|F_{++}^{M_n M_0}|^2 + |F_{+-}^{M_n M_0}|^2). \quad (69)$$

In the derivation of the relations for the polarization, asymmetry, depolarization, and the spin flip we can use results of the general theory of particle polarization.[54]

The proton polarization P, in the case of unpolarized incident protons, takes the form

$$\frac{d\sigma}{d\Omega}(\theta) \cdot P(\theta)\,\mathbf{n} = \frac{1}{(2s+1)(2I_0+1)} 2\,\mathrm{Im} \sum_{M_n M_0} F_{++}^{M_n M_0^*} F_{+-}^{M_n M_0}, \quad (70)$$

where **n** is a unit vector perpendicular to the scattering plane.

We define the analyzing ability as the azimuthal asymmetry of the scattered protons in the case of a fully polarized incident beam:

$$A(\theta) = \mathrm{Tr}(F\sigma F^+)/\mathrm{Tr}(FF^+). \quad (71)$$

The analyzing ability can be expressed in the following manner:

$$\frac{d\sigma}{d\Omega}(\theta) \cdot A(\theta) = \frac{(-1)}{(2s+1)(2I_0+1)} 2\,\mathrm{Im} \sum_{M_n M_0} (-1)^{M_n - M_0} \times F_{++}^{M_n M_0} F_{+-}^{-M_n - M_0^*}. \quad (72)$$

As shown in ref. 55, in the case of elastic scattering of nucleons by unpolarized nuclei, owing to the invariance of the scattering amplitude to time reversal, the polarization (70) coincides with the analyzing ability (72). Therefore, by measuring the asymmetry in elastic scattering, we determine by the same token also the polarization.

We can obtain similarly a relation for the depolarization parameter:

$$D = \mathrm{Sp}(\sigma F \sigma F^+)/\mathrm{Sp}(FF^+) \quad (73)$$

and for the spin-flip probability. The latter, as will be shown later, is connected with the depolarization by the simple relation

$$S = (1 - D)/2; \quad (74)$$

$$S(\theta) = \frac{1}{2} \times \left\{ 1 - \frac{\sum_{M_n M_0} (-1)^{M_n - M_0} \mathrm{Re}\,(F_{++}^{M_n M_0} F_{++}^{-M_n - M_0^*} + F_{+-}^{M_n M_0} F_{+-}^{-M_n - M_0^*})}{\sum_{M_n M_0} (|F_{++}^{M_n M_0}|^2 + |F_{+-}^{M_n M_0}|^2)} \right\}. \quad (75)$$

From A. Bohr's theorem (67) and from (68) we easily see that the spin-flip probability is equal to zero in elastic scattering. Nonetheless, a small value of the spin flip may result from violation of the applicability of Bohr's theorem, e.g., in spin–spin interaction.

One can propose also a more illustrative method of determining all the measured quantities. So far all the equations have been written out here in a coordinate system with the axis z directed along the incident beam. We introduce a different coordinate system, where the z axis is perpendicular to the reaction plane. We denote the proton spin projections on this axis by plus or minus, depending on the direction of the spin of the incident proton (first superscript) and the outgoing proton (second superscript). It is then easy to express $d\sigma/d\Omega$, P, A, D, and S in terms of the partial cross sections:

$$d\sigma/d\Omega = \sigma = \sigma^{++} + \sigma^{+-} + \sigma^{-+} + \sigma^{--}; \quad (76)$$
$$\sigma P = \sigma^{++} + \sigma^{-+} - \sigma^{+-} - \sigma^{--}; \quad (77)$$
$$\sigma A = \sigma^{++} + \sigma^{+-} - \sigma^{-+} - \sigma^{--}; \quad (78)$$
$$\sigma D = \sigma^{++} - \sigma^{+-} + \sigma^{--} - \sigma^{-+}; \quad (79)$$
$$\sigma S = \sigma^{+-} + \sigma^{-+}. \quad (80)$$

The last two relations lead directly to (74).

The partial cross sections can be expressed in terms of the amplitudes (21) after changing over to a new coordinate system, i.e., after rotation through the Euler angles $(\pi/2, \pi/2, \pi)$. Owing to the rotation of the coordinate system, the spherical function $Y_{l_n m_n}(\theta, \varphi)$ in (21) should be replaced by the product $Y_{lm}^{*}(-\pi/2\pi) Y_{l_n \tilde{m}_n}(\pi/2, \theta)$, where the tilde designates a projection in a coordinate system with z axis perpendicular to the reaction plane.[1)]

Interaction in the Generalized Optical Model of Inelastic Scattering

Interaction potential. To describe the experimental data on elastic and inelastic scattering of protons with an excitation of low-lying levels of even–even rare-earth nuclei, we used the generalized optical model[3-5] in all the calculations presented in the present paper.

Low-lying levels of even–even heavy nuclei have a clearly pronounced collective nature and can be explained as states resulting from the presence of static or dynamic deformation of the nuclei. Then the phenomenological description of the inelastic-scattering process can be represented as excitation of vibrations or rotations of the nucleus by the incident particle. Whereas the optical model was used for the case with elastic scattering, in this case a natural generalization is to assume that the optical potential is not spherical. As in the usual optical

model of elastic scattering, we assume that the radial dependence of the interaction is described by a Woods–Saxon potential.[48] Then the potential of the interaction of the particle and the nucleus takes the following form in the spherical coordinate system:

$$V(r,\ \theta,\ \varphi) = -\frac{V}{1+\exp[(r-R)/a]} - \frac{iW}{1+\exp[(r-R_i)/a_i]} - 4i\frac{W_s \exp[(r-R_i)/a_i]}{\{1+\exp[(r-R_i)/a_i]\}^2} - v_{s.o}(r,\ \theta,\ \varphi) + V_{Coul}(r,\ \theta,\ \varphi), \quad (81)$$

where V is the depth of the real potential, W is the depth of the volume-absorption potential, W_S is the depth of the surface-absorption potential, R and a are the radius and diffuseness of the real potential, Ri and a_i are the radius and diffuseness of the imaginary potentials, $v_{S.O}$ is the spin–orbit potential, and V_{Coul} is the Coulomb potential.

The nonsphericity of the potential, i.e., the dependence on the angles θ and φ, appears as the consequence of the assumption that the surface is deformed. For vibrational states of spherical nuclei, the deviation of the radius R or R_i from the spherical-shape radius R_0 can be expanded in multipoles by introducing the dynamic-deformation parameters $\alpha_{\lambda\mu}$:

$$R - R_0 = R_0 \sum_{\lambda\mu} \alpha_{\lambda\mu} Y_{\lambda\mu}(\theta,\ \varphi); \quad (82)$$

$$R_i - R_{0i} = R_{0i} \sum_{\lambda\mu} \alpha_{\lambda\mu} Y_{\lambda\mu}(\theta,\ \varphi). \quad (83)$$

The analogous relations for an axially-symmetric deformed nucleus are

$$R - R_0 = R_0 \sum_{\lambda} \beta_\lambda Y_{\lambda 0}(\theta'); \quad (84)$$

$$R_i - R_{0i} = R_{0i} \sum_{\lambda} \beta_\lambda Y_{\lambda 0}(\theta'), \quad (85)$$

where θ' is the angle in the coordinate system fixed in the nucleus, and β_λ are the deformation parameters. We introduce radial parameters with the aid of the relations

$$R_0 = r_0 A^{1/3}; \quad R_{0i} = r_{0i} A^{1/3}. \quad (86)$$

The possibilities admit of distinguishing between the radii of the real and imaginary parts of the potential, since the absorption and scattering of the particle can occur at different distances. At the same time, the radial parameters of the volume and surface absorption potentials are assumed to be equal.

Spin – orbit dependence of the potential. In certain earlier papers, the spin–orbit potential is given, even in the case of deformed nuclei, in the form

$$\tilde{v}_{s.o} = -\left(\frac{\hbar}{m_\pi c}\right)^2 (\sigma \cdot l)\frac{1}{r}\cdot\frac{dV(r,\ \theta,\ \varphi)}{dr}, \quad (87)$$

where m_π is the pion mass. However, as is clear from the fundamental principles for introducing the spin–orbit potential,[57] expression (87) is valid only for a spherically-symmetric potential V(r). Allowance for the possible deformation of the spin–orbit dependence of the interaction potential assumes the so-called complete Thomas form:

$$v_{s.o} = \left(\frac{\hbar}{m_\pi c}\right)^2 \sigma \left[\frac{1}{i}\nabla \cdot \nabla (V_{s.o}(r,\ \theta,\ \varphi))\right], \quad (88)$$

where

$$V_{s.o}(r,\ \theta,\ \varphi) = (V_{s.o} + iW_{s.o})\{1+\exp[(r-R_{s.o})/a_{s.o}]\}^{-1}. \quad (89)$$

In accordance with Eqs. (82) and (84), we represent $R_{S.O}$ for the vibrational and rotational models in the form

$$R_{s.o} - R_{0s.o} = R_{0s.o} \sum_{\lambda\mu} \alpha_{\lambda\mu} Y_{\lambda\mu}(\theta,\ \varphi); \quad (90)$$

$$R_{s.o} - R_{0s.o} = R_{0s.o} \sum_{\lambda} \beta_\lambda Y_{\lambda 0}(\theta'); \quad (91)$$

$$R_{0s.o} = r_{0s.o} A^{1/3}. \quad (92)$$

The first calculations of inelastic scattering of protons, using a spin–orbit potential of the complicated form (88), were made by Sheriff and Blair.[58] It was shown in some subsequent papers that a correct allowance for the spin–orbit dependence of the potential, when proton scattering is considered with excitation of collective levels, leads to an improved agreement with the experimental data on the asymmetry and on the spin-flip probability. Therefore all the calculations in the present paper with allowance for spin–orbit interaction were performed with a potential of the type (88).

As shown by trial calculations, allowance for absorption in the spin–orbit potential (89) does not lead to any qualitative changes and alters very little the depth, radius, and diffuseness ($V_{S.O}$, $R_{S.O}$, $a_{S.O}$) of the real part of the spin–orbit potential. We shall therefore henceforth put $W_{S.O} = 0$.

Interaction of the incident proton with the Coulomb field of the nucleus. The Coulomb interaction of charged particles of medium energy (up to 100 MeV) with heavy nuclei is quite significant in the elastic- and inelastic-scattering channels. It suffices to note that at small scattering angles (< 20°) the elastic-scattering cross section practically coincides with the Rutherford cross section. In the inelastic-scattering channels there is an appreciable contribution of Coulomb excitation, the role of which increases strongly with decreasing energy of the incident particles, and this makes it necessary to allow for it more accurately at low energies. The interference of the Coulomb and nuclear scattering also assumes great significance at low energies.

The nonrelativistic Coulomb interaction can be represented in the form[46]

$$V_{Coul} = ZZ_N e^2 \int \rho(r',\ \theta',\ \varphi')(|\mathbf{r}-\mathbf{r}'|)^{-1} d\mathbf{r}' = 4\pi ZZ_N e^2 \sum_{\lambda\mu} \int \rho(r',\ \theta',\ \varphi')(2\lambda+1)^{-1} \times r_<^{\lambda} r_>^{-(\lambda+1)} Y_{\lambda\mu}(\theta,\ \varphi)\, Y^*_{\lambda\mu}(\theta',\ \varphi')(r')^2 dr'\, d\Omega', \quad (93)$$

where Z and Z_N are the charges of the incident particle and the nucleus; $\rho(r', \theta', \varphi')$ is the distribution of the charge in the target nucleus, while $r_>$ and $r_<$ are the larger and smaller of the quantities r and r'.

At incident-particle energies greatly exceeding the Coulomb barrier, a sufficiently good approximation for the distribution of the charge of the nucleus is a distribution with sharp edge, i.e., a constant density inside a sphere with Coulomb radius $R_C(\theta', \varphi')$ and zero outside this sphere:

$$\rho_0(r', \theta', \varphi') = 3\theta(R_c(\theta', \varphi') - r')/4\pi R_C^3, \quad (94)$$

where $\theta(\Delta r) = 1$ at $\Delta r > 0$; $\theta(\Delta r) = 0$ at $\Delta r < 0$.

However, as will be shown later on, when the calculations are compared with the experimental data, at energies near the Coulomb barrier it is necessary to determine more precisely the charge distribution in the nucleus. It is reasonable to choose a Fermi distribution of the charge in the nucleus:

$$\rho_F(r', \theta', \varphi') = N\{1 + \exp[(r' - R_C(\theta', \varphi'))/a_C]\}^{-1}, \quad (95)$$

where

$$N = \left[4\pi \int_0^\infty \{1 + \exp[(r - R_C)/a_C]\}^{-1} r^2\, dr\right]^{-1}. \quad (96)$$

By analogy with the nuclear and spin–orbit potentials, we introduce the Coulomb-potential deformation parameters in the vibrational and rotational models with the aid of the following relations:

$$R_C - R_{0C} = R_{0C} \sum_{\lambda\mu} \alpha_{\lambda\mu} Y_{\lambda\mu}(\theta, \varphi); \quad (97)$$

$$R_C - R_{0C} = R_{0C} \sum_{\lambda} \beta_\lambda Y_{\lambda 0}(\theta'); \quad (98)$$

$$R_{0C} = r_{0C} A^{1/3}. \quad (99)$$

Determination of the scattering length. As a result of a comparison of the calculations of the inelastic scattering in accordance with the generalized optical model with the experimental data, the radial parameters for all the terms of the potential turn out as a rule to be slightly different. As already noted, the reason for this may lie in the difference between the physical processes that correspond to the different parts of the optical potential. The deformations of individual parts of the potential then also turn out to be different. Let us examine this question in greater detail using as an example the real and imaginary potentials in the model of an axially-symmetric nucleus having only quadrupole deformation. We conclude from (81), (84), and (85) that the real and imaginary potentials are functions of the following type:

$$U(r, \theta) = U\{r - R_0(1 + \beta_2 Y_{20}(\theta))\}; \quad (100)$$

$$W(r, \theta) = W\{r - R_{0i}(1 + \beta_2 Y_{20}(\theta))\}. \quad (101)$$

Consequently the equipotential surfaces of each of the potentials

$$r - R_0 - R_0\beta_2 Y_{20}(\theta) = \text{const}; \quad (102)$$

$$r - R_{0i} - R_{0i}\beta_2 Y_{20}(\theta) = \text{const} \quad (103)$$

will have different deformations if at $R_0 \neq R_{0i}$ the parameters β_2 in (100) and (101) are chosen to be the same. If we assume the physically more justified point of view that all the parts of the generalized optical potential (81) should have the same deformation, then Eq. (10) must be presented in the form

$$W(r, \theta) = W\{r - R_{0i}(1 + (\beta_2 R_0/R_{0i}) Y_{20}(\theta))\}. \quad (104)$$

Thus, when the deformation parameter β_2 is chosen for the real part of the potential, the corresponding parameter for the imaginary potential is $\beta_2 R_0/R_{0i}$. In the general case, for each potential we have the following equality:

$$\beta_\lambda R_0 = \text{const}. \quad (105)$$

This quantity is called in some papers the scattering length. We note also that it is meaningful to compare not the deformations obtained from different experiments, but the scattering lengths $\beta_\lambda R_0$.

Multipole expansion of potentials. It would be quite difficult to carry out numerical calculations with a potential of the type (81) and with relations (82) taken into account. It is therefore meaningful to use physically justified means of simplifying the expression for the potential.

Obviously, for subsequent calculation of the matrix elements it would be useful to represent the potential in the form of a multipole expansion. At small values of the deformation parameter one can find the coefficients of the multipole expansion of the potential by expanding it in a Taylor series in powers of $(\sum_{\lambda\mu} \alpha_{\lambda\mu} Y_{\lambda\mu}$ or $(\sum_\lambda \beta_\lambda Y_{\lambda 0})$. We present by way of example expressions obtained for the multipole expansion coefficients in the presence of constant quadrupole and hexadecapole deformations with allowance for second-order terms:

$$\tilde{V}_0 = V(r - R_0) + \frac{1}{4\pi} \cdot \frac{\partial V}{\partial r} R_0\beta_2^2 + \frac{1}{8\pi} \frac{\partial^2 V}{\partial r^2} R_0\beta_2^2 + O(\beta_2\beta_4); \quad (106)$$

$$\tilde{V}_2 = -\frac{\partial V}{\partial r} R_0\beta_2 + \frac{1}{7}\sqrt{\frac{5}{4\pi}} \frac{\partial^2 V}{\partial r^2} R_0^2\beta_2^2 + O(\beta_2\beta_4); \quad (107)$$

$$\tilde{V}_4 = -\frac{\partial V}{\partial r} R_0\beta_4 + \frac{1}{7}\sqrt{\frac{9}{4\pi}} \frac{\partial^2 V}{\partial r^2} R_0^2\beta_2^2 + O(\beta_2\beta_4). \quad (108)$$

We see that the expression for the diagonal part contains, in addition to the usual spherically-symmetric potential, also a correction of second order in β_2.

The general expressions for the expansion in the Taylor series in the case of the vibrational model, with allowance for the second-order terms $(\sum_{\lambda\mu} \alpha_{\lambda\mu} Y_{\lambda\mu})^2$, are

given in the paper of Tamura.[4]

As shown by our calculations, when applying the vibrational model to heavy nuclei it suffices to use only the first-order terms in the expansion of the potential. Indeed, the deformation parameters are sufficiently small for phonon excitations of the heavy nuclei.

Large quadrupole-deformation parameters are present in heavy deformed nuclei. In this case, allowance for second-order terms in (106)-(108) may turn out to be insufficient. However, it is precisely when the rotational model is used that one can obtain the multipole-expansion coefficients for the potential with allowance for all the orders in the deformation. These coefficients are defined by the relation

$$v_\lambda(r) = \int V(r - R(\Omega))\, Y_{\lambda 0}(\Omega)\, d\Omega = 4\pi \int_0^1 V(r - R(\theta))\, Y_{\lambda 0}(\cos\theta)\, d(\cos\theta). \tag{109}$$

Numerical integration is possible, since the deformation parameters β_λ are ordinary numbers. As a result, each coefficient $v_\lambda(r)$ is the sum of an infinite number of Taylor-series terms. Unfortunately, it is impossible to use a similar procedure for the vibrational model, since the $\alpha_{\lambda\mu}$ are operators.

In any case, in the generalized optical model one can separate the diagonal part of the interaction V_{diag}, which enters in the homogeneous equations (39) for determination of the distorted waves, and the part of the interaction V_{coup} which is responsible for the transitions between the states.

We emphasize that when the rotational model is used in accordance with relations (84) and (85), the multipole expansion of the potential is carried out in a coordinate system fixed in the nucleus. To change over to the spatial coordinate frame one use the relation

$$Y_{\lambda 0}(\theta') = \sum_\mu D^\lambda_{\mu 0}(\theta_i)\, Y_{\lambda\mu}(\theta, \varphi), \tag{110}$$

where the Euler angles θ_i determine the orientation of the nucleus in space; the functions D are used for the transformation between the coordinate systems.

Calculation of the matrix elements. The transition matrix elements defined by (11) and contained in the system of coupled equations (10) can be calculated by using a multipole expansion of the potential and the wave functions of the chosen collective model of the nucleus.

Following refs. 3 and 4, we can write down a multipole expansion of the potential, in the general case, by separating an operator that acts only on the internal variables ξ of the nucleus:

$$V_{coup}(\mathbf{r}, \xi) = \sum_{\lambda\mu} v_\lambda(r)\, T_{\lambda\mu}(\xi)\, Y_{\lambda\mu}(\theta, \varphi). \tag{111}$$

For example, it follows from the foregoing analysis that in the rotational model the operator is $T_{\lambda\mu}(\xi) \sim D^\lambda_\mu(\theta_i)$ and in the vibrational model, when the potential is expanded in terms of the deformations up to first order, we have $T_{\lambda\mu}(\xi) \sim \alpha_{\lambda\mu}$.

The matrix elements (11) can be expressed in terms of the reduced matrix elements $\langle I \| T_\lambda \| I_1 \rangle$ defined by the relation

$$\langle I \| T_\lambda \| I_1 \rangle = \frac{(2I+1)}{(I_1 \lambda M_1 \mu \mid IM)} \langle \chi_{IM} \mid T_{\lambda\mu}(\xi) \mid \chi_{I_1 M_1} \rangle. \tag{112}$$

We present this general relation, which is derived in Tamura's paper:[4]

$$V^I_{ljl,\, I_1 j_1 l_1} = \sum_\lambda v_\lambda(r) \langle I \| T_\lambda \| I_1 \rangle \frac{1}{\sqrt{4\pi}} (-1)^{J-s-I_1+l+l_1+(l_1-l)/2} \times \sqrt{2l+1}\sqrt{2l_1+1}\sqrt{2j+1}\sqrt{2j_1+1}\,(ll_1 00 \mid \lambda 0) \times W(jIj_1I_1;\, J\lambda)\, W(ljl_1j_1;\, s\lambda). \tag{113}$$

The presented matrix elements can be obtained with the aid of collective models of the nucleus. For the experimental data discussed in the present paper, it suffices to consider the simplest model, namely the vibrational model with excitation of single-phonon states and the axially-symmetric rotator model. Using the corresponding wave functions, with the aid of Eq. (112), we obtain[4] for transitions from the ground state to the single-phonon states of the vibrational model

$$\langle 0 \| T_\lambda \| I \rangle = \delta_{\lambda I} (-1)^I \beta_\lambda, \tag{114}$$

where the parameter β_λ in the vibrational model was introduced in such a way that $\beta^2 = \langle 0 | \sum_\mu |\alpha_\mu|^2 | 0 \rangle$, i.e., it is the expectation value of $\sum_\mu |\alpha_\mu|^2$ in the ground state.

A similar calculation for the rotational model in the presence of axial symmetry yields

$$\langle I \| T_\lambda \| I_1 \rangle = \sqrt{2I+1}\sqrt{2I_1+1}\,(I_1 \lambda K 0 \mid IK). \tag{115}$$

Notice should be taken of an important circumstance observed by Buck:[3] The diagonal matrix elements of the potential V_{coup} vanish in first order in $\alpha_{\lambda\mu}$ for the vibrational model, i.e.,

$$\langle I \| T_\lambda \| I \rangle = 0. \tag{116}$$

This is a result of the fact that the interaction (111) in the vibrational model can cause transitions only between states that differ by one or several phonons. At the same time, in the rotational model the analogous matrix elements differ from zero, and they can be calculated from Eq. (115). This suggests that the results of calculations by the vibrational model will differ from those by the rotational model. However, as shown by numerical calculations, this difference comes into play only at appreciable deformations. A detailed analysis of the results of these numerical calculations will be carried

out in the comparison of the experimental data.

Adiabatic Approximation

In the calculation of inelastic scattering of particles by deformed nuclei, under conditions when the particle energy greatly exceeds the nuclear excitation energies, one can use the adiabatic approximation. The first to use it in the scattering problem was S. I. Drozdov.[5] Under the indicated condition, in the zeroth approximation, the Hamiltonian of the target nucleus, which in this case is the nuclear-rotation energy operator, can be omitted from Eq. (1). Then the asymptotic wave function takes the form

$$\Psi_{\text{asympt}} = \{\exp(ikz) + \exp(ikr)\,\mathcal{F}(\theta, \varphi, \theta_i)/r\}\,\chi_{IKM}(\theta_i), \quad (117)$$

where $\chi_{IKM}(\theta_i)$ is the wave function of the ground state of the target nucleus; θ_i are the Euler angles and determine the orientation of the nucleus; $\mathcal{F}(\theta, \varphi, \theta_i)$ is the amplitude for scattering by an stationary nucleus. Since the nucleus is assumed to be fixed during the scattering, it is clear that the expansion of the complete wave function Ψ does not contain a summation over the scattering channels corresponding to different states of the target nucleus. In other words, the angular momenta In and j are not coupled. Thus, the expansion of the complete function can be expressed in the form[4]

$$\Psi = \sum_{ljk_j} f_{ljk_j}(r)\,\Phi'_{ljk_j}, \quad (118)$$

where the prime labels the coordinate system connected with the nucleus, and k_j is the projection of the total angular momentum of the incident nucleon for the partial wave.

When the coordinate system connected with the nucleus is used, it is possible to avoid a coupling between different partial waves having different values of k_j. The system of coupled equations (10) can then be rewritten in the form

$$[-T_r - V_{\text{coup}} + E]\,f_{ljk_j}(r) = \sum_{l'j'} \langle \Phi'_{lik_j} | V_{\text{coup}} | \Phi'_{l'j'k_j} \rangle\, f_{l'j'k_j}. \quad (119)$$

Thus, in the adiabatic approximation the system of coupled equations becomes much simpler. Since the nucleus is stationary, which implies neglect of its angular momentum in the scattering process, all the scattering channels are taken into account in the system (119).

An appreciable part of the calculations of the present paper was made in the adiabatic approximation. Indeed, the condition for applicability of the approximation is[5]

$$kR\,(\Delta E/E) \ll 1, \quad (120)$$

where k is the wave number of the incident particle, R is the nuclear radius, ΔE is the excitation energy of the nuclear level, and E is the energy of the incident particle. This condition is satisfied for excitation of the levels of the rotational band of the ground state of strongly deformed heavy nuclei at incident-proton energies higher than 10 MeV.

3. COMPARISON OF THEORY WITH EXPERIMENT

In this section we consider the analysis of experimental data[6-8] on inelastic scattering of 12-MeV and 24.5-MeV protons by rare-earth nuclei. The results obtained by other workers at[10] 16 MeV and also on the scattering of α particles[16,17] and deuterons will be discussed in the next section.

Although calculations based on use of the approximate methods for taking second-order effects into account[37,38] play an important role when it comes to finding correct analysis methods, the calculations considered below were obtained using the KASTOR computer program and the program of the sucessive-approximations method.[39] It has been verified that in order for the solution of the latter program to converge it is necessary to use not more than two iterations at parameter values typical of rare-earth nuclei, and this solution practically coincides with the result of the exact numerical solution of the system of coupled equations.

Analysis of the Scattering of 12-MeV Protons by Sm Nuclei

The angular distributions for elastic scattering of protons and for inelastic scattering with excitation of the levels 2^+(0.082 MeV), 4^+(0.267 MeV), and 6^+(0.542 MeV) of ^{154}Sm nuclei, obtained in ref. 6, were calculated in accordance with a program for exact numerical solution in the adiabatic approximation, using a nonspherical optical potential.[60] The spin–orbit dependence was neglected in the calculations, inasmuch as it has been verified that allowance for this dependence changes the calculated cross sections for the elastic scattering of 12-MeV protons and for the inelastic 2^+ and 4^+ scattering only by several per cent at angles less than 150°. The cross section with excitation of the 6^+ level changes more strongly, but the experimental errors incurred in its determination are large.[2)] As expected, the adiabatic approximation introduces a small error only in the calculated cross sections of the highest excited level 6^+ in ^{154}Sm. It turned out that at an incident-proton energy 12 MeV there is no need for introducing volume absorption into the optical potential. Therefore all the calculations were performed with allowance for surface absorption only.

The search for the best parameters for proton scattering by ^{154}Sm nuclei was made by least squares simultaneously for the experimental data on the angular distributions of the elastic scattering and inelastic scattering with excitation of the levels 2^+, 4^+, and 6^+ of the rotational band. Preliminary calculations have shown that the uncertainty in choice of the depth of the real part of the potential and of the radial parameter, which is present in the analysis of elastic scattering only,[1] remains also in the calculation of the cross sections by the strong-coupling method. The radial parameter r_0 can be varied in the approximate range from 1.16 to 1.23 F, and a suitable change of the depth of the potential can yield a prac-

tically constant value of χ^2. For convenience in the comparison of the reduction of the experimental results, the radial parameter was chosen to be $r_0 = 1.204$ as in ref. 61, where the data at 16 MeV were analyzed. The value $r_{0i} = 1.243$ was also kept constant during the course of the reduction.

Since the energy of the incident protons is close to the height of the Coulomb barrier for the Sm nuclei, the distribution of the charge in the nucleus was taken into account more accurately than in earlier studies. The distribution took the form of a Fermi distribution (95) with a diffuseness equal to the diffuseness of the real potential. The numerical integration for the multipole expansion of the Coulomb potential took into account all the orders in the expansion in powers of the quadrupole deformation. When the rotational model was used, a similar multiple expansion was carried out for the other parts of the nonspherical optical potential.

In this program, only fourth-order terms could be taken into account in the multipole expansion of the potential. The next (sixth-order) coefficient, however, contains a term proportional to $(\partial^2 V/\partial r^2)\, R_0^2 \beta_2^2$, and makes a contribution at large values of β_2, expecially to the cross section for the excitation of the 6^+ level. Therefore, after finding the best values of the optical-potential and deformation parameters, as indicated in Table 1, the cross section for scattering with excitation of the 6^+ level was calculated in accordance with the successive-approximations program, which includes the next higher terms of the expansion.

A comparison with the experimental data is shown in Fig. 1, which gives also the results of the calculation with a sharp-edge nuclear charge distribution at the same values of the remaining parameters. As seen from the figure, the greatest change occurs in the cross section for scattering with excitation of the 2^+ level. Compensation can be obtained only by increasing β_2 by approximately 15%. Thus, the use of the more justified Fermi distribution is quite important at 12-MeV proton energy. The accuracy with which the deformation parameters have been determined is about 10%.

To calculate the scattering of 12-MeV protons by ^{148}Sm nuclei, the same optical-potential parameters were used as for ^{154}Sm (see Table 1), and only the quadrupole-deformation value was chosen by least squares. A value $\beta_2 = 0.13$ was obtained. As seen from Fig. 2, the experimental theoretical angular distributions are in sufficiently good agreement.

The signs of the deformation parameters were determined quite reliably. By way of illustration, Fig. 3

TABLE 1. Optical-Potential and Deformation Parameters for Scattering of 12-MeV Protons by ^{154}Sm Nuclei

Potential	Potential depth, MeV	Radial parameter, F	Diffuseness parameter, F	Deformation
V	56.7	1.204	0.741	β_2=0.284
W_s	8.62	1.243	0.629	β_4=0.046
V_{Coul}	—	1.204	0.741	

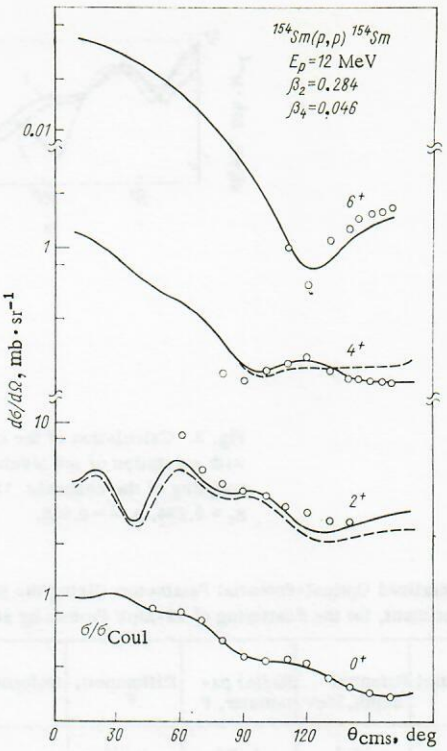

Fig. 1. Angular distributions of elastic and inelastic scattering of 12-MeV protons by ^{154}Sm nuclei: circles – experimental data; solid curve – calculation with Fermi charge distributions; dashes – calculation with sharp edge.

shows the results of the calculations of the cross sections for inelastic scattering of protons with excitation of the 2^+ and 4^+ levels for various chosen combinations of the signs of the parameters β_2 and β_4. We see that the first of these cross sections is more sensitive to the sign of β_2 and the second to the sign of β_4.

Estimate of the Spin-Flip Probability in Inelastic Scattering

The small value of the spin-flip probability in inelastic scattering of 12 MeV protons with excitation of the

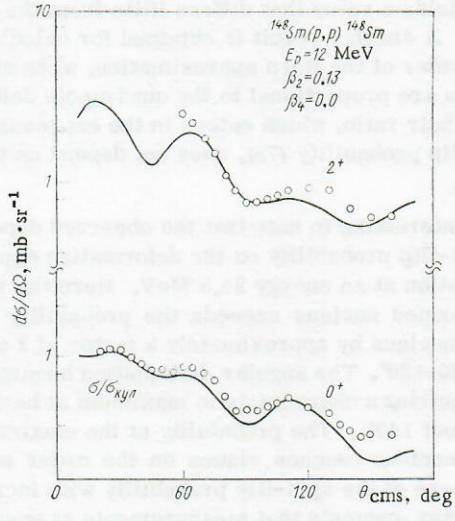

Fig. 2. Angular distributions of elastic and inelastic scattering of 12-MeV protons by ^{148}Sm nuclei: circles – experimental data; solid curves – calculation with Fermi charge distribution.

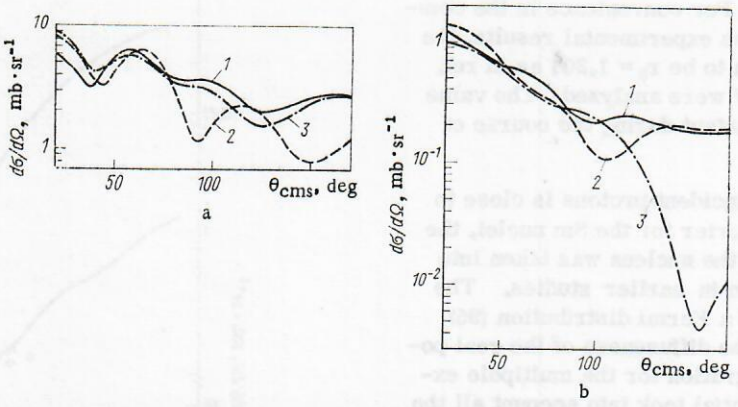

Fig. 3. Calculation of the cross section for inelastic scattering of 12-MeV protons with excitation of the levels 2^+ (a) and 4^+ (b) of ^{154}Sm by the method of the strong coupling of the channels: 1) $\beta_2 = 0.284$, $\beta_4 = 0.046$; 2) $\beta_2 = -0.284$, $\beta_4 = 0.046$; 3) $\beta_2 = 0.284$, $\beta_4 = -0.046$.

TABLE 2. Generalized Optical-Potential Parameters Giving the Best Agreement with Experiment, for the Scattering of 12-MeV Protons by Sm Nuclei

Nucleus	Potential	Potential depth, MeV	Radial parameter, F	Diffuseness, F	Deformation
^{154}Sm	V	56.7	1.204	0.741	$\beta_2 = 0.28 \pm 0.02$
	W_s	8.6	1.243	0.63	$\beta_3 = 0.06 \pm 0.02$
	$V_{s.o}$	6	1.06	0.74	
^{148}Sm	V	60	1.204	0.741	$\beta_2 = 0.126 \pm 0.01$
	W_s	8.6	1.243	0.63	$\beta_3 = 0.155 \pm 0.01$
	$V_{s.o}$	6	1.06	0.74	

first 2^+ levels of the Sm nuclei[7] is evidence of a small contribution of spin–orbit forces to the scattering amplitude. For scattering by ^{148}Sm, experiment yields at all angles a spin-flip probability equal to zero, with an error of 2-3%. Calculation of the spin-flip probability by the method of coupled channels with the parameters of Table 2 also offers evidence of a low spin-flip probability, giving a value that varies little with variation of the proton-scattering angle.

Experiment reveals that the spin-flip probability increases for the deformed nucleus ^{152}Sm. However, calculation yields a value that differs little from the result for ^{148}Sm. A similar result is obtained for calculation in the first order of the Born approximation, when all the amplitudes are proportional to the quadrupole deformation, and their ratio, which enters in the expression for the spin-flip probability (75), does not depend on the deformation.

It is interesting to note that the observed dependence of the spin-flip probability on the deformation appears in the calculation at an energy 24.5 MeV. Here the result for a deformed nucleus exceeds the probability for a spherical nucleus by approximately a factor of 2 at angles near 90-120°. The angular distribution becomes anisotropic, acquiring a characteristic maximum at backward angles (about 160°). The probability at the maximum for a deformed nucleus reaches vlaues on the order of 0.4. This increase of the spin-flip probability with increasing proton energy suggests that measurements at energies near 20 MeV and higher would be useful for the study of the spin–orbit interaction of a proton with a deformed target nucleus.

Excitation of Octupole Vibrations in Sm Nuclei in Inelastic Scattering of 12-MeV Protons

We analyze here the obtained angular distributions of inelastically scattered protons with excitation of the 3^- levels of ^{148}Sm and ^{154}Sm. The presence of these levels in the nuclei is attributed to the existence of octupole surface vibrations. They were first observed in the study of electromagnetic transitions of E3 type, which have a high probability. The reduced probabilities B(E3) of the electromagnetic transitions and the parameters β_3 of the octupole deformation were determined in studies of Coulomb excitation in the scattering of various charged particles of energy lower than the Coulomb barrier by nuclei.[62] With increasing energy of the incident charged particles an appreciable role is assumed, besides the Coulomb excitation process, also by the nuclear interaction, which likewise leads to excitations of octupole vibrations in the nuclei.

A possible calculation method at small values of the deformation is the first-order distorted-wave Born approximation. However, as will be shown below, allowance for the channel coupling for the quadrupole and octupole excitations can greatly alter the results of the calculation.

For an appreciable number of rare-earth isotopes, Elbek and co-workers measured the inelastic scattering of deuterons at 12 MeV with excitation of octupole states.[62,63] The measurements were performed, however, at two or three scattering angles, making the analysis difficult.

Calculations using the vibrational model were carried out in accordance with the program of the successive-approximations method.[64] Inasmuch as the 3^- states have a relatively high excitation energy (1.162 MeV for ^{148}Sm and 1.011 MeV for ^{154}Sm), the nonadiabaticity of the process was taken into account. The deformation of the real spin–orbit part of the potential was chosen in accordance with the complete Thomas form. The small contribution of the excitation of the two-phonon state 4^+ (1.181 MeV) of the ^{148}Sm nucleus, which cannot be resolved from the 3^- level, was neglected. It is shown in ref. 65 that this contribution does not exceed 10% of the cross section.

The coupling of the 3^- channel with the elastic-scattering channel is small, and allowance for the 3^- channel

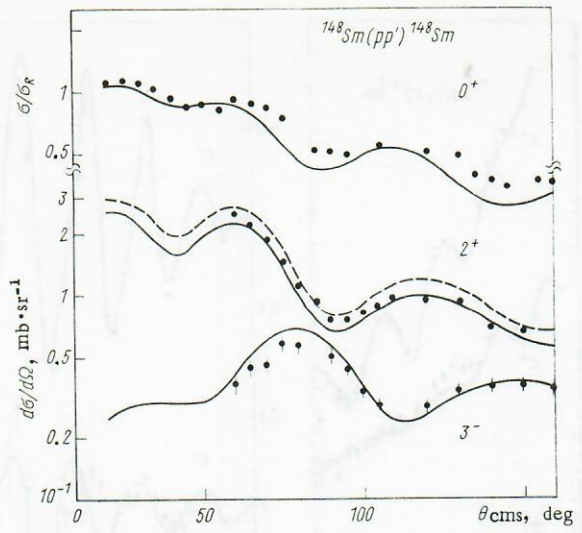

Fig. 4. Angular distributions of elastic and inelastic scattering of 12-MeV protons by ^{148}Sm nuclei: circles – experimental data: solid curves – calculation with the set of parameters of Table 2; dashed curves – the same set of parameters, but $\beta_2 = 0.14$.

alters little the elastic-scattering cross section. Nonetheless, a simultaneous analysis of the 0^+, 2^+, and 3^- channels can change the calculation parameters, since the angular distribution of the protons inelastically scattered with excitation of the 3^- depends essentially on the choice of the optical-potential parameters.

Indeed, calculation with allowance for the coupling of the 0^+, 2^+, and 3^- channels carried out for ^{148}Sm with the set of optical-potential parameters of Table 1, $\beta_2 = 0.13$ and $\beta_3 = 0.15$ results in poor agreement with the experimental 3^- cross section. This set of parameters was determined above from the analysis of only the 0^+ and 2^+ channels, and resulted in fair agreement with experiment, when account was taken of the Fermi smearing of the potential.

Considerable improvement in comparison with the data on all three channels can be obtained, as seen from Fig. 4, by slightly increasing (by 3 MeV) the depth of the real potential and choice of the deformation parameters $\beta_2 = 0.126$ and $\beta_3 = 0.155$. Account was taken also of the spin–orbit dependence of the potential. The parameters are given in Table 2. The observed deviation of the calculated curve for the elastic-channel scattering can be attributed to inaccuracy of the absolute normalization of the measured cross section.

The investigation of the excitation of octupole states of the nonspherical nucleus ^{154}Sm is a much more complicated task. The excited state 3^- (1.011 MeV) occurs in a rotational band of negative parity 1^-, 3^-, 5^-, etc. The wave functions of the nucleus should take into account the possibility of octupole vibrations of the nonspherical surface.[66] Calculations with these functions have not yet been carried out, owing to the considerable complication of the calculations. The difference between the angular distributions of elastic scattering and inelastic scattering with excitation of the 2^+ level, calculated in accordance with the rotational and vibrational models, is small. An attempt was therefore made to estimate the effect of the nonsphericity of the nucleus, i.e., of the presence of the deformation β_2, on the octupole vibrations by carrying out the calculation in accordance with the purely vibrational model with the optical-potential parameters from Table 2. Qualitative agreement is obtained at an octupole-deformation parameter value 0.06 ± 0.02.

Analysis of the Scattering of Polarized 24.5-MeV Protons by ^{148}Sm and ^{152}Sm Nuclei

The availability of data on the analyzing ability of elastically and inelastically scattered protons makes it possible to increase greatly the accuracy with which the optical-potential parameters and the deformation parameters are determined. The angular dependences of the analyzing ability are strongly oscillating curves, the shape of which depends not only on the parameters of the spin–orbit potential, but is determined to a considerable degree also by all the remaining parameters.

A theoretical description of the experimental data[8] was carried out with the aid of the nonadiabatic program of the successive-approximations method.[39] The deformation of the real spin–orbit part of the potential was taken into account in the complete Thomas form. Corrections were introduced for the values of the deformations of different parts of the potential, in order to ensure equality of the scattering length βR for different radial parameters.

Calculations of the angular distributions of the cross sections and of the asymmetry of the elastic scattering of protons by the spherical nuclei ^{148}Sm and of inelastic scattering with excitation of the levels 2^+ (0.551 MeV) and 3^- (1.162 MeV) were carried out using the vibrational model with allowance for the coupling of all three channels. As indicated earlier, the contribution of the experimentally nonresolved two-phonon 4^+ (1.181 MeV) state could be neglected.[65]

The rotational model was used for the scattering of protons by ^{152}Sm nuclei. Account was taken here of the coupling of four states, namely 0^+, 2^+ (0.122 MeV), 4^+ (0.366 MeV), and 6^+ (0.712 MeV) which, as assumed, make up the rotational band of the ground state. Although scattering with excitation of the 6^+ state was not measured in the experiment, it was shown that allowance for this state noticeably alters the calculated values of the cross section and the asymmetry for the state 4^+.

The results of preliminary calculations have shown that the ambiguity in the choice of the geometrical parameters of the real part of the potential V and r_0 decreases if the data for the analyzing ability of the inelastic scattering are taken into account at the same time. In analysis of only the elastic-scattering channel, as shown in ref. 1, this ambiguity is more significant, since the parameter r_0 can range from 1.14 to 1.20 F. Calculations were carried out with the parameter sets listed in Table 3. They have shown that although the elastic-scattering cross section and the polarization are equally well described by these parameter sets, to describe the analyzing ability of the inelastic scattering it is preferable to choose $r_0 = 1.2$ F. Only at this value does a maximum appear at backward angles in the angular dependence of the analyzing ability when the 2^+ level is excited.

TABLE 3. Trial Values of the Optical-Potential Parameters for the Scattering of Protons by ^{148}Sm Nuclei (β_2 = 0.12)

Potential	Potential depth, MeV	Radial parameter, F	Diffuseness parameter, F
V	50	1.22	0.74
W	3	1.25	0.63
W_s	9	1.25	0.63
$V_{s.o}$	6	1.06	0.74
V	53	1.20	0.74
W	3	1.24	0.67
W_s	8	1.24	0.67
$V_{s.o}$	6	1.01	0.74
V	56	1.18	0.74
W	3	1.22	0.63
W_s	9	1.22	0.63
$V_{s.o}$	6	1.06	0.74

The set of parameters obtained by simultaneous analysis of the scattering in the channels 0^+, 2^+ and 3^-, with allowance for the coupling, is given in Table 4 (set 3). A comparison of the calculation with the experimental data is shown in Fig. 5. An attempt was made to describe the data for proton scattering by ^{152}Sm nuclei, by using the same optical-potential parameters as for ^{148}Sm. It was assumed in this case that the quadrupole deformation is increased, a hexadecapole deformation was introduced, and the vibrational model was replaced by the rotational model with coupling of the channels 0^+, 2^+, 4^+, and 6^+. In Fig. 6, the results of this trial calculation with β_2 = 0.25 and B_4 = 0.07 are represented by a dashed curve. We see that although it was possible to describe the observed oscillation-damping effect for the analyzing ability of the inelastic scattering with excitation of the 2^+ level, the general agreement is not satisfactory.

The best agreement was obtained by slightly modifying the optical-potential parameters (see Fig. 6, solid curve). The parameters are listed in Table 4 (set 7).

As seen from Figs. 5 and 6, the calculations by the coupled-channel method account for the most characteristic difference between the analyzing abilities of inelastic scattering of protons with excitation of the 2^+ levels of ^{148}Sm and ^{152}Sm. The differences in the scattering of protons by spherical and deformed nuclei will be considered in greater detail later on.

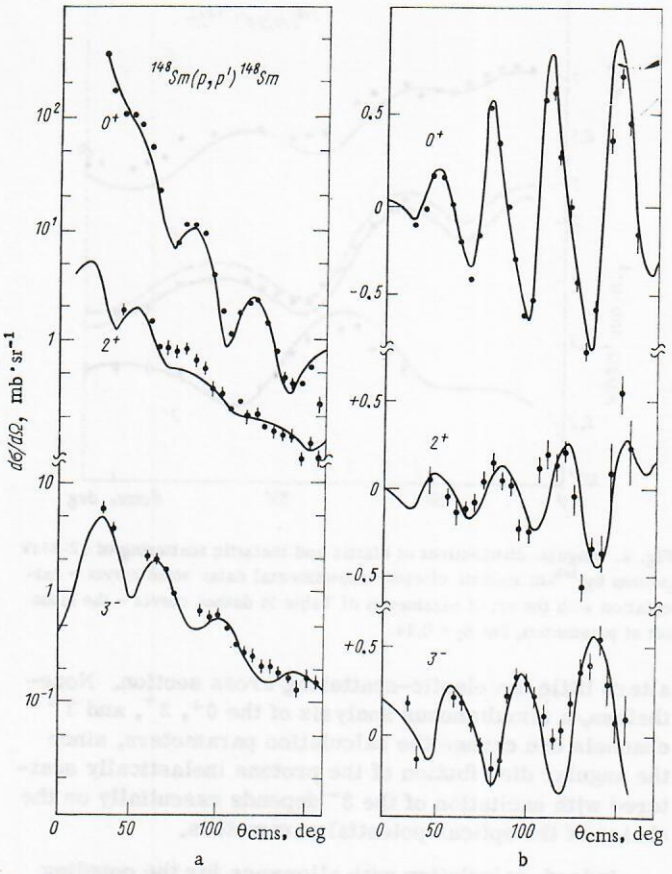

Fig. 5. Angular distributions of the cross sections (a) and of the analyzing ability (b) of elastic and inelastic scattering of 24.5-MeV polarized protons by ^{148}Sm nuclei. The solid curves show calculations with the vibrational model.

Possibility of Determining the Form of the Collective Excitation of Nuclei

An interesting distinguishing feature of the method of analyzing elastic scattering with allowance for strong coupling of the channels is the possibility of identifying the vibrational or rotational structure of the states of the nuclei. In those cases when a rotational band corresponding to the ground state is observed for the target nuclei, the foregoing analysis of the inelastic scattering of protons, as well as of α particles[17] and of deuterons,[20] confirms the conclusion that a constant deformation is present in the surface of these nuclei. However, if the energy distribution of the low-lying levels of nuclei does not per-

TABLE 4. Parameters of the Optical Potential of Samarium Nuclei for the Scattering of Protons with Various Energies

Set	Target nucleus	E, MeV	V, MeV	r_0, F	a, F	W, MeV	W_s, MeV	r_{0i}, F	a_i, F	$V_{s.o}$ MeV	$r_{0s.o}$, F	$a_{s.o}$, F	r_{0C}, F	β_2	β_3	β_4	Reference
1	^{148}Sm	12	60	1.204	0.741	0	8.6	1.243	0,63	6	1.06	0.74	1.21	0.126±0.01	0.155±0.01	—	[64]
2		12	57.6	1.204	0.72	0	11.8	1.295	0.62	6.2	1.05	0.75	1.21	—	—	—	[1]
3		24.5	54	1.2	0.74	2.5	8.5	1.22	0,67	5.2	1.01	0.74	1.21	0.12±0.01	0.15±0.01	—	[8]
4		24.5	53.6	1.2	0.72	2.2	8.7	1.30	0,62	6.2	1.05	0.75	1.21	—	—	—	[1]
5		49.5	46.55	1.168	0.816	5.73	3,45	1.36	0.63	5.61	1.075	0,816	1.21	—	—	—	[69]
6		49.5	47.4	1.17	0,75	8.2	1,4	1,32	0,623	6.2	1.01	0,75	1,21	—	—	—	[1]
7	^{152}Sm	24.5	48	1,2	0,74	1,2	8,5	1,37	0.67	5.2	1.01	0,74	1.21	0.250±0.01	—	0.07±0.02	[8]
8		24.5	54	1.2	0.72	2.2	8.9	1.30	0.64	6.2	1.05	0,75	1,21	—	—	—	[1]
9*	^{154}Sm	12	56,7	1,204	0.741	0	8,62	1,243	0.629	—	—	—	1.204	0.284±0,01	0.06±0.02	0.046±0.02	[60]
10		12	58.2	1.204	0.72	0	12.2	1.295	0,646	6.2	1.05	0.75	1.21	—	—	—	[1]
11		16	54.03	1.204	0,715	0	7.5	1.243	0,667	—	—	—	1.204	0.25	—	0.05	[61]
12		16	56.8	1.204	0,72	0	11	1.295	0,646	6.2	1.05	0.75	1.21	—	—	—	[1]

* This set of parameters was obtained through a calculation with a Fermi distribution of the charge and α_C = 0.74.

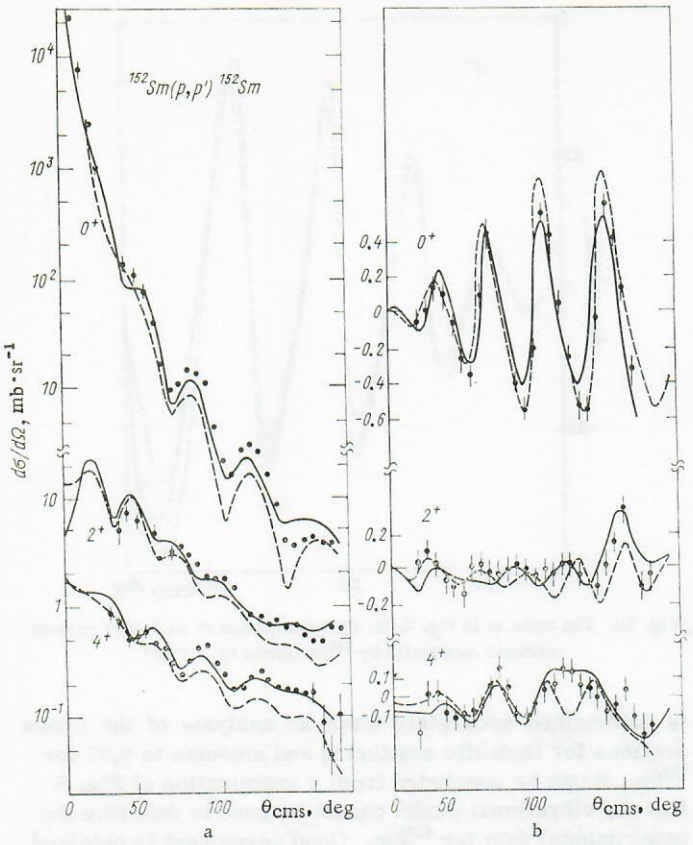

Fig. 6. Angular distributions of the cross sections (a) and of the analyzing ability (b) of elastic and inelastic scattering of 24.5-MeV polarized protons by ^{152}Sm nuclei:[11] dashed curves – calculation with rotational model and the optical-potential parameters obtained for ^{148}Sm; solid curves – calculation with those parameters of Table 4 which give the best agreement with the experimental data.

mit a clear-cut conclusion concerning the applicability of the simple vibrational or rotational model, as is the case, e.g., in the transition-nuclei region near A = 150 and A ~ 190, the question arises of the possibility of using data on only the first 2^+ levels of even–even nuclei to determine the form of the collective excitation of the nuclei.

As noted earlier,[3] there is a fundamental difference between the diagonal elements calculated in accordance with the rotational and vibrational models. For the rotational model, one can use the equation (115):

$$\langle I \| T_2 \| I \rangle = (2I+1)\,(I\,200\,|\,I0), \qquad (121)$$

whereas in the vibrational model, the analogous diagonal elements are equal to zero [Eq. (116)]. The off-diagonal quadrupole matrix elements coincide in first-order expansion in the deformation parameter.

The difference between the elastic- and inelastic-scattering cross sections calculated in accordance with different models was pointed out in ref. 3. This difference, however, is small and can be offset by varying the optical-model parameters. The experimentally observed[6,9,17] considerable difference between the cross sections for elastic and inelastic scattering of protons and α particles by spherical and deformed Sm nuclei is due mainly to enhancement of the coupling of the channels, owing to the increase in the value of the deformation parameter on going to deformed nuclei.

As noted first in ref. 8, the angular dependence of the analyzing ability in inelastic scattering of 24.5-MeV protons with excitation of the first 2^+ levels of the Sm nuclei is quite sensitive to the form of the collective model used in the calculations with the coupled channels.

We present below the results of calculations of elastic and inelastic scattering of 24.5-MeV protons by ^{152}Sm nuclei; these results illustrate the possibilities of the proposed method of determining the form of the collective excitation of the nuclei.[67] The calculations were carried out in accordance with the program of the method of successive approximations.[39] To describe the 2^+ state, a vibrational or axially-symmetric rotational model was used with set 3 of the optical-potential parameters of Table 4. Two values of the quadrupole-deformation parameter were used, 0.115 and 0.25, which are close respectively to the typical values of the dynamic and static deformations of the rare-earth nuclei.

The results of calculation of the analyzing ability for a lower value of the deformation are shown in Fig. 7. It is seen that the calculations in accordance with the vibrational and rotational models yield results that are close, and the experimental data on the scattering of protons by ^{148}Sm nuclei can be explained within the limits of errors by using either model. The calculations reveal a weak sensitivity to the diagonal quadrupole matrix element (121) at a small value of the deformation parameter. Consequently, allowance for the quadrupole moment observed in ref. 25 for the 2^+ state does not lead to disagreement with experiment, since the corresponding matrix element is of the same order as (121) in the rotational model with $\beta_2 = 0.115$.

At a quadrupole-deformation parameter value 0.25, a considerable difference is observed between the angular

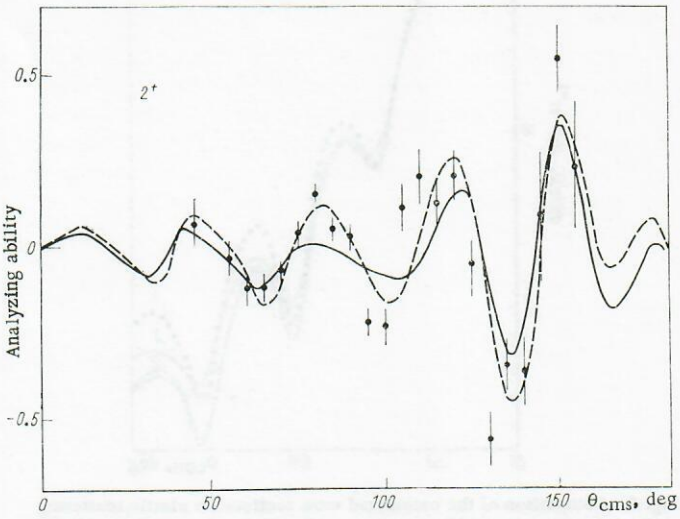

Fig. 7. Angular dependence of the analyzing ability for inelastic scattering of polarized 24.5-MeV protons by Sm nuclei with excitation of the first 2^+ level: circles – experimental data for ^{148}Sm (ref. 8); dashed curves – results of calculations by the coupled-channel method using the vibrational model; solid curve – calculation by the rotational model with axial symmetry. The optical-potential parameters are indicated in Table 4 (set 3), and $\beta_2 = 0.115$.

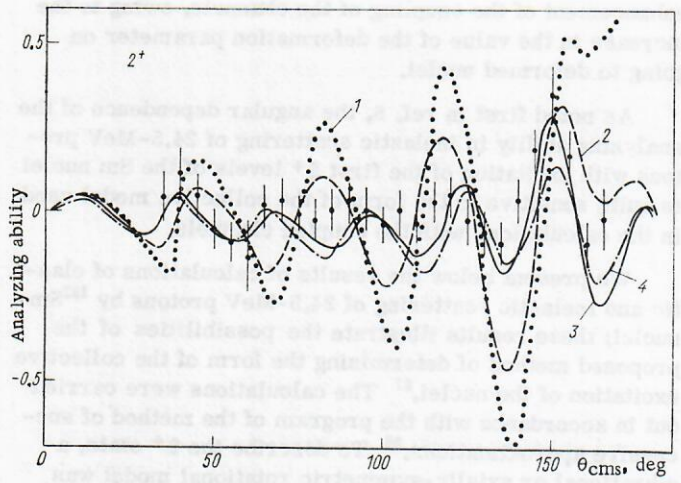

Fig. 8. Angular dependence of the analyzing ability for inelastic scattering of polarized 24.5-MeV protons by Sm nuclei with excitation of the first 2^+ level. The black circles show the experimental data for ^{152}Sm (ref. 11); 2) calculation in accordance with the vibrational model; 3) calculation in accordance with the rotational model with axial symmetry, with allowance for the coupling of the 0^+ and 2^+ channels; 4) with allowance for the coupling of the 0^+, 2^+, and 4^+ channels. The optical-potential parameters are indicated in Table 4 (set 3), $\beta_2 = 0.25$; 1) calculated in accordance with the rotational model at $\beta_2 = -0.25$.

dependences of the analyzing ability of (2^+) as calculated by the vibrational and rotational models. The oscillations in the angular dependence of the analyzing ability in the case of the rotational model are strongly smoothed out in comparison with the calculation by the vibrational model, and in the latter case there is practically no dependence on the value of the deformation parameter. Since β_2

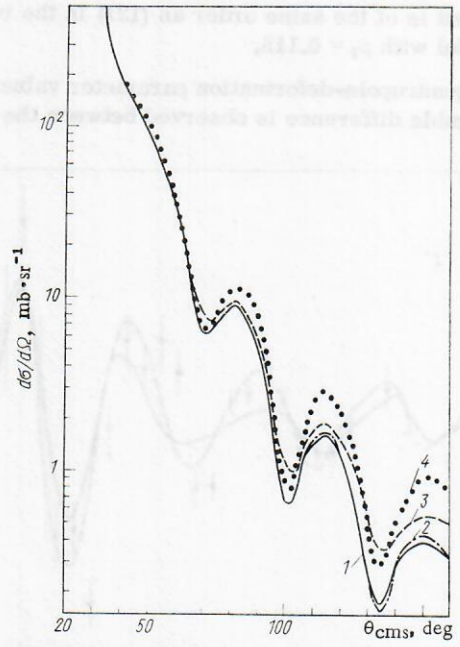

Fig. 9. Comparison of the calculated cross sections for elastic scattering of 24.5-MeV protons by ^{152}Sm nuclei: 1) in accordance with the rotational model with allowance for the influence of the 2^+ channel of energy 0.122 MeV; 2) with allowance for the influence of channels 2^+ and 4^+ with energy 0.367 MeV; 3) in accordance with the vibrational model $(0^+, 2^+)$ at a deformation $\beta_2 = 0.25$; the optical-model parameters are indicated in Table 4 (set 3); 4) calculation in accordance with the vibrational model at $\beta_2 = 0.115$.

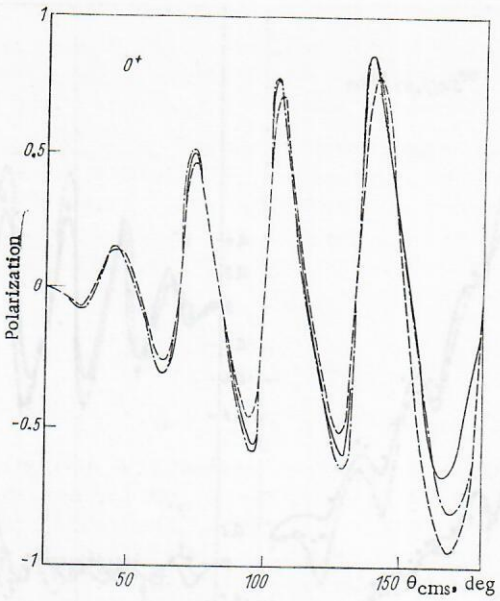

Fig. 10. The same as in Fig. 9, for the polarization of 24.5-MeV protons scattered elastically by ^{152}Sm nuclei ($\beta_2 = 0.25$).

is determined accurately from an analysis of the cross sections for inelastic scattering and amounts to 0.25 for ^{152}Sm, it can be concluded from a examination of Fig. 8 that the vibrational model cannot be used to describe the experimental data for ^{152}Sm. Good agreement is obtained only by using the rotational model with the large value $\beta_2 = 0.25$. A calculation carried out with a negative value of the deformation (see Fig. 8) determines in addition the sign of the deformation and makes it possible, apparently, at large values of the deformation, to distinguish between the applicability of the rotational and vibrational models by using the data on the analyzing ability, if the state 2^+ has a negative quadrupole moment.

For comparison, Figs. 9-11 show the results of calculation of the cross sections and polarization at $\beta_2 = 0.25$. The difference between the results of the calculations by different models is not so large as for the analyzing ability, and cannot be used to identify the model. At a lower value of the deformation parameter, the curves practically coincide. It is seen from Fig. 9 that the increase of the oscillations in the angular distribution of

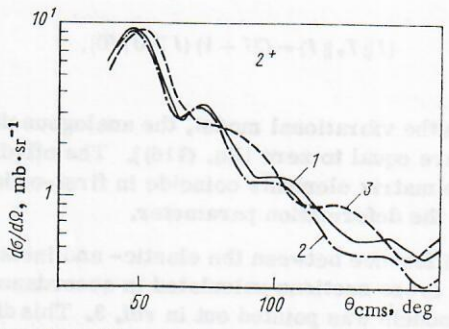

Fig. 11. Comparison of the calculated cross section for inelastic scattering of 24.5-MeV protons by ^{152}Sm nuclei: 1) in accordance with the rotational model with allowance for the coupling of the channels 0^+ and 2^+ with energy 0.122 MeV; 2) with allowance for the coupling of the channels 0^+, 2^+, and 4^+ with energy 0.367 MeV; 3) in accordance with the vibrational model $(0^+, 2^+)$ at a deformation $\beta_2 = 0.25$.

the elastic-scattering cross section, as calculated by the vibrational model with $\beta_2 = 0.115$ and observed in experiment,[6] is due mainly to the smaller value of the deformation parameter.

Thus, measurement and analysis of the angular distribution of the analyzing ability of inelastic scattering of protons with excitation of the state 2^+ make it possible to determine the collective nature of this state under the condition that the deformation parameter exceeds a value on the order of 0.15.

4. EFFECTIVE POTENTIAL AND CHARGE DISTRIBUTION IN THE NUCLEUS

Optical-Potential Parameters

From the foregoing comparison of the theoretical calculations with the experimental data it follows that the generalized optical model, when account is taken of the strong coupling of the channels, describes adequately the angular dependence of the cross sections, of the polarization, and of the analyzing ability for elastic and inelastic scattering of medium-energy protons by rare-earth nuclei.

The most complete analysis of elastic scattering polarization of protons in accordance with the optical model with a spherically symmetric potential was carried out in ref. 1. At the same time, certain average parameters of the optical potential were determined for an appreciable number of data on elastic scattering of protons by nuclei with $A > 40$ at energies less than 50 MeV, using least squares. To obtain the best agreement it is necessary to introduce an energy dependence of the depth parameters of the real and imaginary potentials, and a dependence on $(N - Z)/A$ was introduced not only into the real potential and the surface-absorption potential, but also into the diffuseness of the imaginary potential.

In the reference[1] cited as well as in many earlier papers, only the data on elastic scattering by spherical nuclei were analyzed. Attempts to analyze elastic scattering by deformed nuclei in accordance with the optical model lead to sets of parameters that differ from those for neighboring nuclei. This difference was observed not only for proton scattering, but also for scattering of deuterons and α particles. It is due to the influence of the coupling of the elastic-scattering channel with the inelastic-scattering channels in the presence of considerable deformation. In first-order approximation, the coupling of the channels can be taken into account by increasing the depth of the imaginary potential. This effect is physically understandable, for if no consistent analysis is made of the channel coupling, the inelastic-scattering channels are equated to the reaction channels and this results in increased absorption; it is to account for this increased absorption that the imaginary potential is introduced.

The expression given by Feshbach[68] for the optical potential contains a sum over all the discarded channels. The consistent allowance which is made in the method of strong coupling of the channels for the effect of certain selected channels with excitation of collective levels on the elastic-scattering channel still does not affect that part of the sum which concerns the region of high excitation of the target nucleus. It can be assumed that this region depends little on the structure of the low-lying levels of the nuclei with different collective properties. Then the optical potential becomes the same for deformed and spherical nuclei after the strongly coupled channels are separated. To the contrary, the observed difference between the parameters of the optical potential can be attributed to a difference in the structure of the highly-excited levels of the nuclei considered.

Table 4 lists the optical-potential parameters of Sm nuclei at different proton energies. We emphasize that the parameters obtained in the present paper were obtained by simultaneously searching for the best description of both the elastic and inelastic scattering with excitation of the most strongly coupled levels of the target nucleus. In ref. 61, at an energy 16 MeV, the parameters were not very carefully chosen. In ref. 69, at a proton energy 49.5 MeV, the analysis for ^{148}Sm was carried out in accordance with the optical model without allowance for the coupling of the channels.

Table 4 indicates, for each set of the parameters, the optical-potential parameters calculated in accordance with the empirical equation of ref. 1, which, as mentioned above, describes elastic scattering by an appreciable number of spherical nuclei at $A > 40$ and $E_p < 50$ MeV. This empirical equation, however, is given for $r_0 = 1.17$ F. A recalculation to the value $r_0 = 1.2$ F was carried out with the aid of the plotted correlation of the parameters (see ref. 1).

The accuracies with which the optical-potential parameters were determined at a given r_0 are approximately

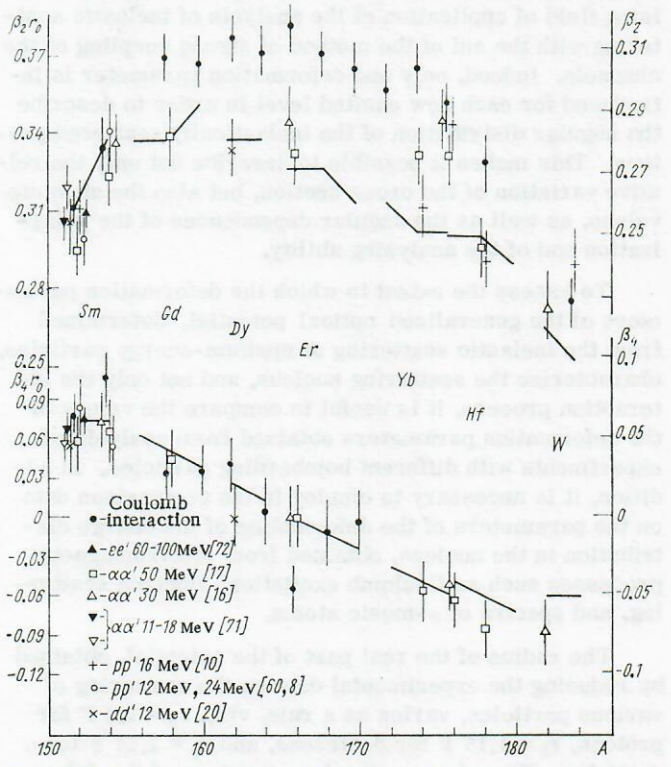

Fig. 12. Comparison of the scattering lengths $\beta_2 r_0$ and $\beta_4 r_0$ and of the deformation parameters referred to $r_0 = 1.2$ F, obtained from an analysis of different experiments for deformed nuclei in the rare-earth region: The straight-line segments are the result of theoretical calculations.[76]

$\Delta V = 0.5$ MeV, $\Delta W = 0.2$ MeV; $\Delta W_S = 0.5$ MeV; $\Delta V_{s.o} = 0.5$ MeV; $\Delta r_i = 0.02$ F; $\Delta a = \Delta a_i = 0.02$ F; $\Delta r_{0s.o} = 0.4$ F using the data on the polarization and asymmetry. The accuracy with which the parameter r_0 is determined from our data is 0.02 F, and the accuracy obtained in ref. 1 using only elastic-scattering data is 0.04 F.

It is seen from Table 4 that the optical-model parameters obtained in the present paper for the spherical nucleus ^{148}Sm agree well with the empirical equation at 24.5 MeV. The small difference in the depth of the potentials at 12 MeV can be attributed to the fact that in ref. 1 they analyzed mainly data obtained at large proton energies. The optical-potential parameters for the deformed nucleus ^{154}Sm differ little from the parameters of the spherical nucleus ^{148}Sm. A slight decrease of the depth of the real part of the potential is observed. The real potential, as well as the volume-absorption potential and the radial parameter of the imaginary part of ^{152}Sm, differ greatly from the corresponding values for the spherical nucleus ^{148}Sm.

It can be proposed that the observed differences between the optical-potential parameters are due to the unaccounted-for coupling with the channels upon excitation of the levels that follow directly the considered low-lying states. Of particular interest is the nucleus ^{152}Sm, which is on the borderline between the spherical and deformed nuclei.

Deformation Parameters of Rare-Earth Nuclei

The determination of the deformation parameters of nuclei, especially of deformed nuclei, is a highly promising field of application of the analysis of inelastic scattering with the aid of the method of strong coupling of the channels. Indeed, only one deformation parameter is introduced for each new excited level in order to describe the angular distribution of the inelastically scattered protons. This makes it possible to describe not only the relative variation of the cross section, but also the absolute values, as well as the angular dependences of the polarization and of the analyzing ability.

To assess the extent to which the deformation parameters of the generalized optical potential, determined from the inelastic scattering of medium-energy particles, characterize the scattering nucleus, and not only the interaction process, it is useful to compare the values of the deformation parameters obtained from analysis of experiments with different bombarding particles. In addition, it is necessary to employ in the comparison data on the parameters of the deformation of the charge distribution in the nucleus, obtained from electromagnetic processes such as Coulomb excitation, electron scattering, and spectra of μ-mesic atoms.

The radius of the real part of the potential, obtained by reducing the experimental data on the scattering of various particles, varies as a rule, viz., $r_0 = 1.2$ F for protons, $r_0 = 1.15$ F for deuterons, and $r_0 = 1.44$ F for α particles. Therefore a direct comparison of the deformation parameters is meaningless. However, as indicated above, comparison of the quantities βR or βr_0 can indicate whether the shapes of the equipotential surfaces are similar or different. The difference between the radii of the potentials and their deviation from the charge radius are attributed to the finite radius of the nucleon–nucleon interaction.[70] The radius of the potential is therefore not a quantity that reflects with sufficient accuracy the distribution of the nuclear mass. At the same time, the shape of the equipotential surface does not depend on the interaction radius and appears to be more sensitive to the distribution of the protons and neutrons in the nucleus, and also to the possible difference between these distributions.

Figure 12 shows, for deformed even–even rare-earth nuclei, the values of the products $\beta_2 r_0$ and $\beta_4 r_0$, taken from studies of the elastic scattering of protons (refs. 8, 10, 60),[3)] deuterons,[20] and α particles,[16,17,71] where the analysis was carried out by the method of strong coupling of the channels. Also shown are data obtained for there nuclei from inelastic scattering of electrons,[72] as well as the scattering lengths $\beta_2 r_0$ and $\beta_4 r_0$ calculated from the measured values of the reduced probabilities of the electromagnetic transitions. The quantities B(E2, $0 \to 2$) and B(E4, $0 \to 4$) were obtained by averaging the data of the review article 73, where measurements of various electromagnetic processes performed up to 1970 are summarized, and are the latest work on Coulomb excitation by heavy nuclei.[21,23,24,27,28] In that case when the values of B(E4, $0 \to 4$) were not measured for the neclei, the corresponding values of the hexadecapole deformation were taken from the inelastic-scattering data.

To determine the deformation parameters, the reduced probabilities of the electromagnetic transitions were calculated:[74]

$$B(E\lambda,\ I_i \to I_f) = \langle I_i \lambda K 0 \mid I_f K\rangle^2 M^2;$$
$$M = Z \int r^2 \rho(r)\, Y_{\lambda 0}(\theta)\, d\tau;$$

for the Fermi charge distribution with allowance for the deviation from spherical symmetry and conservation of the volume we have

$$\rho(r) = \rho_0 \{1 + \exp[(r - R_C(\theta))/a_C]\}^{-1};$$
$$R_C(\theta) = r_{0C} A^{1/3} [1 + \beta_2 Y_{20}(\theta) + \beta_4 Y_{40}(\theta) - \beta_2^2/4\pi].$$

The values $r_{0C} = 1.1$ F and the diffuseness of the charge distribution $a_C = 0.54$ F were taken to be close to the values obtained for the investigated region of nuclei from the data on electron scattering[72] and on mesic atoms.[75]

The deformation parameters shown in Fig. 12 satisfy simultaneously the experimental values of B(E2) and B(E4). The accuracies of the points indicated in the figure are worse by a factor of several times than the accuracy of B(E2) cited in the experimental papers (about 1%), owing to the considerable error in the determination of B(E2) and to allowance for the contribution of the hexadecapole deformation to the value of B(E2).

It follows from an examination of Fig. 12 that the data on the scattering lengths for different scattered particles agree well enough with one another. Good agreement between the data on scattering and on the electromagnetic processes is observed also at the start and end

of the region, but the discrepancy between them is quite appreciable in the middle of the region. Unfortunately, the data on the particle scattering is quite scanty here. To be able to affirm more definitely that the shapes of the equipotential surfaces of the charge distribution and of the nuclear potential are different for the isotopes of Gd, Dy, and Er it is desirable to perform additional measurements. Of particular interest is measurement of inelastic scattering in the region of the Coulomb barrier, when the parameters of the nonspherical optical potential and of the charge distribution are determined simultaneously,[71] and to perform the measurements with a beam of polarized protons, so as to improve the accuracy with which the parameters are determined.[8,11]

The straight lines in Fig. 12 join the results of the latest theoretical calculations of equilibrium deformation with single-particle levels of a Woods–Saxon potential.[76] They agree well with the data on particle scattering and emphasize an interesting feature of rare-earth nuclei, namely that the hexadecapole deformation parameter changes from 0.05 at the start of the region to −0.05 at its end.

In conclusion, let us compare the various methods of determining nuclear deformation. The methods using Coulomb excitation of the nuclei and the investigation of the x-ray spectra of μ-mesic atoms employ a small number of parameters of the theory, in fact only the parameters of the Fermi charge distribution. It is therefore possible to determine with good accuracy the quantities making the main contribution to the transition probability, i.e., the quadrupole-deformation parameters. Consequently, it is possible to observe small effects, such as the quadrupole moment of the excited states,[25,26] and deviations from the rigid-rotator model for the ^{152}Sm nucleus.[27] At the same time, when inelastic scattering is analyzed with allowance for the strong coupling of the channels, one does not encounter the suppression of the higher-order transitions, which is observed in electromagnetic processes, even though the accuracy with which the quadrupole deformation parameter is determined is worse because of the presence of a large number of optical-potential parameters. For example, the determination of the hexadecapole deformation parameter, which is a small effect in the Coulomb-excitation method,[23,24] depends very strongly on the assumed rigidity of the nucleus, In inelastic nuclear scattering of heavy particles, the contribution of the direct transition to the excitation of the high-spin levels is more appreciable, and it is possible to determine more accurately the parameters of the hexadecapole deformation and even of deformation of higher order.[8,17,60] There are expectations that inelastic scattering of electrons may be useful for the determination of deformation parameters.[72]

The coupled-channel method for the scattering of strongly interacting particles makes it possible to determine the signs of the deformation parameters, something impossible in the Coulomb-excitation method.[4)] A study of of inelastic scattering of polarized protons and analysis with allowance for the strong coupling of the channels at parameter values $\beta_2 > 0.15$ yields information on the static or dynamic nature of the deformation.

[1)]We note that the sign of the amplitude in ref. 56 is in error.

[2)]Some of the calculations are repeated below without the use of the adiabatic approximation, and with allowance for the spin–orbit dependence of the potential.

[3)]The results of the analysis of ref. 61, where the calculations were preliminary, are not given here.

[4)]See ref. 26, where it is shown that measurement of the correlation of the scattered particles and of the γ radiation in Coulomb excitation makes it possible to determine the sign of the quadrupole moment of the excited 2^+ state.

[1]F. D. Becchetti and G. W. Greenlees, Phys. Rev., 182, 1190 (1969).
[2]D. M. Chase, L. Wilets, and A. R. Edmonds, Phys. Rev., 110, 1080 (1958).
[3]B. Buck, A. P. Stamp, and P. E. Hodgson, Phil. Mag., 8, 1005 (1963).
[4]T. Tamura, Rev. Mod. Phys., 37, 679 (1965).
[5]S. I. Drozdov, Yad. Fiz., 1, 407 (1965); 2, 810 (1965) [Sov. J. Nucl. Phys. 1, 290 (1965); 2, 578 (1966)].
[6]A. B. Kurepin, B. Madsen, and B. Élbek, Izv. AN SSSR, Ser. Fiz., 31, 195 (1967).
[7]A. B. Kurepin, P. R. Christensen, and N. Trauther, Nucl. Phys., A115, 471 (1968).
[8]A. B. Kurepin and R. M. Lombard, Phys. Lett., B37, 55 (1971).
[9]P. Stoler et al., Phys. Rev., 155, 1334 (1967).
[10]T. Kruse et al., Nucl. Phys., A169, 177 (1971).
[11]M. P. Barbier et al., Phys. Lett. B34, 386 (1971).
[12]J. M. Moss et al., Phys. Rev. Lett., 26, 1488 (1971).
[13]L. L. Gol'din, G. I. Novikova, and K. A. Ter-Martirosyan, Zh. Eksp. Teor. Fiz., 36, 512 (1958) [Sov. Phys.–JETP, 9, 356 (1958)].
[14]K. Kjallquist, Nucl. Phys., 9, 163 (1958).
[15]M. G. Huber, Phys. Lett., 13, 242 (1964).
[16]A. A. Aponick et al., Nucl. Phys., A159, 367 (1970).
[17]D. L. Hendrie et al., Phys. Lett., B26, 127 (1968).
[18]B. Zeidman et al., Nucl. Phys., 86, 471 (1966).
[19]G. Løvhøiden, B. Skaali, and P. R. Christensen, Phys. Lett., B34, 125 (1971).
[20]N. Trautner, G. Løvhøiden, and P. R. Christensen, Phys. Lett., B44, 41 (1973).
[21]R. E. Sayer et al., Phys. Rev., C1, 1525 (1970).
[22]F. S. Stephens et al., Phys. Rev. Lett., 24, 1137 (1970).
[23]F. S. Stephens, R. M. Diamond, and J. de Boer, Phys. Rev. Lett., 27, 1151 (1971).
[24]K. A. Erb et al., Phys. Rev. Lett., 29, 1010 (1972).
[25]J. J. Simpson et al., Nucl. Phys., A94, 177 (1967).
[26]L. Grodzins et al., Phys. Lett., 30, 453 (1973).
[27]R. M. Diamond et al., Phys. Rev., C3, 344 (1971).
[28]R. M. Diamond et al., Nucl. Phys., A184, 481 (1972).
[29]R. Beurtey, Proc. Second Intern. Symp. on Polarization Phenomena of Nucleons, Karlsruhe, Birkhäuser Verlag, Basel (1966), p. 33.
[30]R. Buertey and J. M. Durand, Nucl. Instr. Meth., 57, 313 (1967).
[31]Yu. G. Basargin, Zh. Tekh. Fiz., 38, 2091 (1968) [Sov. Phys.–Tech. Phys., 13, 1677 (1969)].
[32]H. G. Blosser et al., Nucl. Instr. Meth., 91, 61 (1971).
[33]C. Chianelli, A. Garin, and B. Waast, Note CEA-N-1522 (1971), p. 147.
[34]G. Dearnaley, A. G. Hardacre, and B. D. Rogers, AERE-R 5813 (1968).
[35]M. Q. Makino et al., Nucl. Instr. Meth., 60, 109 (1968).
[36]A. B. Kurepin, Tr. FIAN SSSR, 69, 3 (1973).
[37]J. M. Bang et al., Nucl. Phys., A122, 34 (1968).
[38]A. B. Kurepin, Izv. AN SSSR, Ser. Fiz., 32, 1946 (1968).
[39]J. Raynal, Nuclear Theory Course, Trieste (1971).
[40]A. Lane and R. Thomas, Theory of Nuclear Reactions at Low Energies [Russian translation], IL (1960).
[41]N. K. Glendenning, Proc. Instern. School of Physics "Enrico Fermi", Course 50, Academic Press, New York (1969).
[42]M. A. Melkanoff, T. Sawada, and J. Raynal, Methods in Computational Physics, Nuclear Physics, Vol. 6, Academic Press, New York–London (1966).
[43]A. S. Davydov, Quantum Mechanics [in Russian], Fizmatgiz, Moscow (1963), p. 422.
[44]M. Goldberger and K. Watson, Collision Theory, Wiley, New York (1962), p. 202.
[45]The Tamm–Dancoff Method, Problemy Sovremennoi Fiz., IL, Moscow (1955), p. 10.
[46]R. H. Bassel, R. M. Drisko, and G. R. Satchler, ORNL-3240 (1962).
[47]G. R. Satchler, Lecture notes, unpublished (1966).

[48]R. D. Woods and D. S. Saxon, Phys. Rev., 95, 577 (1954).
[49]P. E. Hodgson, The Optical Model of Elastic Scattering [Russian translation], Atomizdat, Moscow (1966).
[50]W. Tobocman, Theory of Direct Nuclear Reactions, Oxford (1961), p. 97.
[51]A. I. Baz', Ya. B. Zel'dovich, and A. M Perelomov, Scattering Reactions and Decay in Nonrelativistic Quantum Mechanics [in Russian], Nauka, Moscow (1971).
[52]A. P. Stamp, Phys. Rev., 153, 1052 (1967).
[53]A. Bohr, Nucl. Phys., 10, 486 (1959).
[54]A. S. Davidov, Theory of the Atomic Nucleus [in Russian], Fizmatgiz (1958).
[55]L. Wolfenstein and J. Ashkin, Phys. Rev., 85, 947 (1952).
[56]D. Robson, Isospin in Nuclear Physics, North-Holland, Amsterdam (1969).
[57]W. Heisenberg, Theorie des Atomkerns, Croninger, Gottingen (1951).
[58]H. Sherif and J. S. Blair, Phys. Lett., B26, 489 (1968).
[59]A. Bohr, Mat.-Fys. Medd. Dan Vid. Selsk., 26, No. 14 (1952).
[60]A. B. Kurepin, H. Schulz, and H. J. Wiebicke, Nucl. Phys., A189, 257 (1972).
[61]P. H. Brown and P. Stoler, Phys. Rev., C2, 765 (1970).
[62]E. Veje et al., Nucl. Phys., A109, 489 (1968).
[63]T. Grotdal et al., Nucl. Phys., A110, 385 (1968).
[64]A. B. Kurepin, Krat. Soobshch. Fiz., FIAN SSSR, No. 3, 22 (1972).
[65]R. A. Kenefick and R. K. Sheline, Phys. Rev., 133, 25 (1964).
[66]A. S. Davydov, Excited States of Atomic Nuclei [in Russian], Atomizdat, Moscow (1967), p. 192.
[67]A. B. Kurepin, R. M. Lombard, and J. Raynal, Phys. Lett., B45, 184 (1973).
[68]H. Feshback, Ann. Phys. (N.Y.), 19, 287 (1967).
[69]P. B. Woolan et al., Nucl. Phys., A154, 513 (1970).
[70]A. Bohr and B. Mottelson, Nuclear Structure, Vol. 1, Benjamin (1969).
[71]W. Brückner et al., Phys. Rev. Lett., 30, 57 (1973).
[72]W. Bertozzi et al., Phys. Rev. Lett., 28, 1711 (1972).
[73]K. E. G. Löbner, M. Vetter, and V. Hönig, Nuclear Data Tables A, Vol. 7 (1970), p. 495.
[74]A. B. Kurepin and N. S. Topil'skaya, Yad. Fiz., 20, 1117 (1974) [Sov. J. Nucl. Phys., 20, No. 6 (1975) (in press)].
[75]D. Hitlin et al., Phys. Rev., C1, 1184 (1970).
[76]D. A. Arsen'ev et al., Izv. AN SSSR, Ser. Fiz., 37, 906 (1973).